Insect Biochemistry and Molecular Biology 110 (2019) 19–33

Contents lists available at ScienceDirect

Insect Biochemistry and Molecular Biology

journal homepage: www.elsevier.com/locate/ibmb

High-resolution QTL mapping in *Tetranychus urticae* reveals acaricide-specific responses and common target-site resistance after selection by different METI-I acaricides

Simon Snoeck[a,1], Andre H. Kurlovs[a,b,1], Sabina Bajda[a], René Feyereisen[a,c], Robert Greenhalgh[b], Ernesto Villacis-Perez[e], Olivia Kosterlitz[b,f], Wannes Dermauw[a], Richard M. Clark[b,d,**], Thomas Van Leeuwen[a,e,*]

[a] Department of Plants and Crops, Faculty of Bioscience Engineering, Ghent University, Coupure links 653, 9000, Ghent, Belgium
[b] School of Biological Sciences, University of Utah, 257 South 1400 East, Salt Lake City, UT, 84112, USA
[c] Department of Plant and Environmental Sciences, University of Copenhagen, Thorvaldsensvej, Copenhagen, Denmark
[d] Center for Cell and Genome Science, University of Utah, 257 South 1400 East, Salt Lake City, UT, 84112, USA
[e] Institute for Biodiversity and Ecosystem Dynamics (IBED), University of Amsterdam (UvA), Science Park 904, 1908 XH, Amsterdam, the Netherlands
[f] Present address: Department of Biology, University of Washington, 24 Kincaid Hall, Seattle, WA, 98195, USA

A B S T R A C T

Arthropod herbivores cause dramatic crop losses, and frequent pesticide use has led to widespread resistance in numerous species. One such species, the two-spotted spider mite, *Tetranychus urticae*, is an extreme generalist herbivore and a major worldwide crop pest with a history of rapidly developing resistance to acaricides. Mitochondrial Electron Transport Inhibitors of complex I (METI-Is) have been used extensively in the last 25 years to control *T. urticae* around the globe, and widespread resistance to each has been documented. METI-I resistance mechanisms in *T. urticae* are likely complex, as increased metabolism by cytochrome P450 monooxygenases as well as a target-site mutation have been linked with resistance.

To identify loci underlying resistance to the METI-I acaricides fenpyroximate, pyridaben and tebufenpyrad without prior hypotheses, we crossed a highly METI-I-resistant strain of *T. urticae* to a susceptible one, propagated many replicated populations over multiple generations with and without selection by each compound, and performed bulked segregant analysis genetic mapping. Our results showed that while the known H92R target-site mutation was associated with resistance to each compound, a genomic region that included cytochrome P450-reductase (CPR) was associated with resistance to pyridaben and tebufenpyrad. Within CPR, a single nonsynonymous variant distinguished the resistant strain from the sensitive one. Furthermore, a genomic region linked with tebufenpyrad resistance harbored a non-canonical member of the nuclear hormone receptor 96 (NHR96) gene family. This NHR96 gene does not encode a DNA-binding domain (DBD), an uncommon feature in arthropods, and belongs to an expanded family of 47 NHR96 proteins lacking DBDs in *T. urticae*. Our findings suggest that although cross-resistance to METI-Is involves known detoxification pathways, structural differences in METI-I acaricides have also resulted in resistance mechanisms that are compound-specific.

1. Introduction

Agrochemicals that inhibit electron transport in the mitochondrial respiratory chain have been commonly and successfully used against phytophagous mites (Lümmen, 2007; Van Leeuwen et al., 2014). These compounds are referred to as Mitochondrial Electron Transport Inhibitors (METIs) and have been classified into groups depending on the site or complex they block. Four large transmembrane complexes (I-IV) mediate electron transport in the mitochondrial inner membrane via several redox reactions from NADPH and FADH2 to oxygen, which serves as the final electron acceptor. An outcome of these sequential redox reactions is the proton gradient that drives ATP synthesis by the F_0F_1 ATPase (complex V) (Karp, 2008). Classic METIs like quinolines, pyridinamines, pyrazoles and pyridazinones act on complex I, the proton translocating NADH: ubiquinone oxidoreductase. This is the largest and most complex multi-subunit structure of the respiratory chain, and it s responsible for catalyzing the electron transfer from NADH to coenzyme Q10 (ubiquinone). These acaricides are referred to

* Corresponding author. postal address: Coupure links 653, 9000 Ghent, Belgium.
** Corresponding author.postal address: 257 S 1400 E, Rm 201, Salt Lake City, UT, 84112, USA.
E-mail addresses: simonp.snoeck@ugent.be (S. Snoeck), andre.kurlovs@ugent.be (A.H. Kurlovs), sabina.bajda@ugent.be (S. Bajda), rene.feyereisen@plen.ku.dk (R. Feyereisen), robert.greenhalgh@utah.edu (R. Greenhalgh), ernestovp85@gmail.com (E. Villacis-Perez), oliviakosterlit@gmail.com (O. Kosterlitz), wannes.dermauw@ugent.be (W. Dermauw), richard.m.clark@utah.edu (R.M. Clark), Thomas.VanLeeuwen@ugent.be (T. Van Leeuwen).
[1] both authors contributed equally.

https://doi.org/10.1016/j.ibmb.2019.04.011
Received 28 February 2019; Received in revised form 8 April 2019; Accepted 13 April 2019
Available online 22 April 2019
0965-1748/

as METI site I or METI-Is, and belong to Insecticide Resistance Action Committee (IRAC) group 21 (Hollingworth et al., 1994; Hollingworth and Ahammadsahib, 1995; Wirth et al., 2016). Although the specific binding sites for ubiquinone and inhibitors may not be identical (Fendel et al., 2008; Tocilescu et al., 2010), inhibition of complex I has been described for many structurally diverse compounds that are thought to interfere with ubiquinone reduction (Degli Esposti, 1998; Lümmen, 1998). Competition experiments have shown that hydrophobic inhibitors of complex I share a common binding domain with at least partially overlapping sites (Okun et al., 1999). Structural data on complex I, as well as biochemical studies (Schuler and Casida, 2001; Shiraishi et al., 2012), support the hypothesis that binding sites for both ubiquinone and inhibitors are comprised of the nuclear-encoded PSST and the 49 kDa subunits of complex I (Fiedorczuk et al., 2016; Vinothkumar et al., 2014; Zickermann et al., 2015). The PSST subunit is the most likely carrier of iron-sulfur cluster N2, a proposed direct electron donor for the ubiquinone reduction (Duarte et al., 2002; Friedrich, 1998; Magnitsky et al., 2002).

Acaricide resistance develops via two main mechanisms: the pharmacokinetic mechanism, which is primarily caused by a decreased exposure due to quantitative or qualitative changes in major detoxification enzymes and transporters, and the pharmacodynamic mechanism, which involves a decrease in sensitivity due to changes in the acaricide's target site (Feyereisen et al., 2015; Li et al., 2007; Van Leeuwen and Dermauw, 2016). These mechanisms are driven by three types of genetic changes (Feyereisen, 2015): (1) mutations that affect the coding sequences of the target gene or detoxification genes, (2) mutations that alter expression levels of target/detoxification genes by affecting *cis* or *trans* regulation, or (3) whole target/detoxification gene duplications or deletions. Combinations of these genetic mechanisms are also possible. For instance, point mutations in acetylcholinesterase that make an organism resistant to organophosphates also decrease the enzyme's effectiveness, leading to gene duplications as a compensation mechanism (Kwon et al., 2010).

Tetranychus urticae (Acari; Tetranychidae), the two-spotted spider mite, is a major crop pest that feeds on over 1000 plant species and has been found on every continent except Antarctica (Migeon et al., 2006–2018). *T. urticae* is notoriously resistant to acaricides and insecticides, with resistance to over 95 active compounds reported to date (Michigan State University, 2018; Van Leeuwen and Dermauw, 2016). Resistance to METI-Is in *T. urticae* was initially documented in the 1990s and has since become widespread (Cho et al., 1995; Devine et al., 2001; Herron and Rophail, 1998; Ozawa, 1994). METI-I resistance in the spider mite was first associated with increased cytochrome P450 (P450) activity by synergism and enzyme activity tests (Cho et al., 1995; Devine et al., 2001; Herron and Rophail, 1998; Ozawa, 1994; Van Pottelberge et al., 2009b), and based on genome-wide microarray gene expression data, a number of constitutively upregulated P450s were identified in METI-I resistant strains. Subsequent studies revealed that one of those upregulated P450s (CYP392A11) metabolized fenpyroximate – but not pyridaben or tebufenpyrad – to a non-toxic metabolite when expressed in *E. coli* (Riga et al., 2015), suggesting that the enzymes involved in METI-I metabolism may vary depending on the acaricide involved. More recently, targeted sequencing and genetic analysis identified a variant in the *T. urticae* PSST homologue of complex I, H92R (*Yarrowia lipolytica* numbering; H110R in *T. urticae*), that appeared to significantly reduce sensitivity to fenpyroximate, pyridaben, and tebufenpyrad (Bajda et al., 2017). This mutation is currently the only known genetic change associated with resistance to METI-I compounds in *T. urticae*. Introgression into a sensitive strain, however, suggested that the mutation explained only a fraction of the total resistance phenotype (Bajda et al., 2017). Additional genetic changes underlying other METI-I resistance mechanisms have so far remained elusive.

The two-spotted spider mite is a tractable organism for characterizing resistance mechanisms, as its haplodiploid breeding system (males are haploid while females are diploid) facilitates inbred line construction, its genome size is small (~90 Mb), the generation time is as little as a week at optimal temperatures, and very large populations can be propagated (Van Leeuwen and Dermauw, 2016). Bulked segregant analysis (BSA) approaches have been used with *T. urticae* to identify monogenic loci (Bryon et al., 2017; Demaeght et al., 2014; Van Leeuwen et al., 2012), and these methods were recently extended to successfully describe polygenic resistance to a lipi synthesis inhibiting acaricide, spirodiclofen (Wybouw et al., 2019). For genetic mapping of resistance with BSA methods, a resistant parent is crossed with a sensitive one, and resultant populations are expanded and selected with the pesticide. In *T. urticae*, BSA studies have used multigenerational populations (which allow dense recombination to break apart haplotypes – a prerequisite for high-resolution mapping), with whole-genome sequencing of parents and derived populations to simultaneously genotype and detect allele frequency changes that identify causal loci (i.e., fixation or increases in the frequency of alleles contributed by the resistant parent).

In this study, we adapted recent advances in BSA methods, and a chromosome-level assembly of the *T. urticae* genome (Wybouw et al., 2019), to comprehensively investigate the quantitative (polygenic) genetic architecture of resistance to the METI-I acaricides fenpyroximate, pyridaben and tebufenpyrad. To do so, we performed multiple rounds of acaricide selection on the offspring of a cross between a Belgian greenhouse strain of *T. urticae* (MR-VP) that exhibited high levels of resistance to these commonly used METI-Is (Van Pottelberge et al., 2009b), and the METI-I-sensitive strain Wasatch (Bryon et al., 2017). As assessed by whole-genome sequencing, multiple quantitative trait loci (QTL) for the three METI-I acaricides were identified, revealing a common target-site mutation and suggesting novel acaricide-specific resistance mechanisms.

2. Materials and methods

2.1. Acaricides

The acaricides used in this study were commercial formulations (Fyto Vanhulle, Belgium) of fenpyroximate (Naja; 50 g a.i. L^{-1} SC), pyridaben (Sanmite; 150 g a.i. L^{-1} SC) and tebufenpyrad (Pyranica; 200 g a.i. L^{-1} SC).

2.2. T. urticae strains

The METI-I resistant strain MR-VP was originally collected in September 2005 from bean plants in a greenhouse at the National Botanical Garden (Brussels, Belgium) (Van Pottelberge et al., 2009b), which had a spray history of tebufenpyrad (Pyranica; 200 g a.i. L^{-1} SC) and pyridaben (Sanmite; 150 g a.i. L^{-1} SC); the strain has since been kept in the laboratory at a constant selection pressure of 1000 mg L^{-1} tebufenpyrad. The susceptible Wasatch strain was originally collected from tomato (*Solanum lycopersicum*) in Salt Lake City, Utah, USA (Bryon et al., 2017), from a public garden where spraying with synthetic pesticides was prohibited. Both strains were mother-son inbred for six generations as previously described (Bryon et al., 2017; Van Petegem et al., 2018). Prior to the experiment, both *T. urticae* strains were maintained under laboratory conditions (25 °C, 60% RH and 16:8 L:D photoperiod) on detached bean leaves (*Phaseolus vulgaris*) resting on cotton pads in plastic boxes to prevent contamination. LC_{50} assays for strains MR-VP and Wasatch were performed as previously described (Van Leeuwen et al., 2004). For each acaricide, LC_{50} values, slopes and 95% confidence limits of the parental strains were estimated using Probit Analysis (PoloPlus version 2.0; LeOra Software, Berkeley, CA, USA). If 5000 mg L^{-1} did not cause 50% mortality, no further attempts were made to determine LC_{50}.

2.3. Experimental evolution set-up of METI-I resistance

An F_1 hybrid population was generated by crossing 22 one-day-old virgin adult females of the inbred Wasatch strain with a single young male of the inbred MR-VP strain. 332 virgin F_1 teliochrysalis females were collected in total and were backcrossed to 70 males of the Wasatch strain. Subsequently, approximately 500 F_2 females were used for the inoculation of potted bean plants, and the resulting segregating bulk populations were kept in a climatic chamber (Panasonic MLR-352H-PE, Kadoma, Japan) at 28 °C with a photoperiod of 16:8 h light:dark for 4–5 generations to expand the population. To set up acaricide selection, 500 individuals from the bulk population were transferred to control plants or those sprayed with 50 mg L^{-1} of either fenpyroximate, pyridaben, or tebufenpyrad; ten replicates were set up for each of the four groups. Experimental evolution on whole bean plants took place in the greenhouse at 21 °C over a period of nine months (~25 generations). When the population size was large enough, mites from each treatment group were transferred to new plants with an increasing concentration of the respective acaricide over time. The concentrations varied depending on the acaricide and were empirically determined based on the efficacy of the previous round of selection. Selection was considered complete when no acaricide-related mortality was observed on beans sprayed until run-off with the final concentrations of 3500, 1250, and 750 mg L^{-1}, for fenpyroximate, pyridaben, and tebufenpyrad, respectively.

2.4. METI-I resistance and adaptation assay

Effectiveness of selection to the three acaricides was evaluated by performing toxicity bioassays as previously described (Van Leeuwen et al., 2004). Mites were grown on unsprayed bean plants for two to four generations, depending on the population size, before conducting toxicity tests. To determine toxicity, approximately 30 gravid adult females were transferred to 9 cm^2 square-cut leaf discs on wet cotton wool and then sprayed with 1 ml of fluid at 1 bar pressure with a Potter Spray Tower (Burkard Scientific, Uxbridge, UK) to obtain a homogenous spray film (deposit of 2 mg cm^{-2}). Each of the ten replicates of the three acaricide-selected populations and the control populations were tested in four replicates at a discriminating concentration of 2500 mg L^{-1} of the relevant acaricide. The leaf disks were kept in a climatically controlled room at 25 °C, 60% RH with a 16:8 h light:dark photoperiod for 24 h. Mites were scored as being alive if they could walk normally after being prodded with a camel's hair brush. Survival percentages of the three acaricide-selected and control populations were analyzed separately using a generalized linear mixed model with a binomial distribution using the lme4 R package version 1.1 (Bates et al., 2015). Here, selection regime was incorporated as a fixed effect in the linear model, while replicate was regarded as a random effect.

2.5. RNA extraction and sequencing

Total RNA was extracted from about 100 adult female mites from the inbred MR-VP strain using the RNeasy Mini Kit (Qiagen, Belgium) with five-fold biological replication. The quality and quantity of the total RNA was analyzed by a DeNovix DS-11 spectrophotometer (DeNovix, Wilmington, DE, USA) and by running an aliquot on a 1% agarose gel. Illumina libraries were constructed from the RNA samples with the TruSeq Stranded mRNA Library Preparation Kit with polyA selection (Illumina, San Diego, CA, USA), and the resulting libraries were sequenced on an Illumina HiSeq 2000 to generate strand-specific paired reads of 2 × 100 bp (library construction and sequencing was performed at Centro Nacional de Análisis Genómico [CNAG], Barcelona, Spain). The RNA reads have been placed in the Sequence Read Archive under accession numbers SAMN11334652 through SAMN11334656.

2.6. DNA preparation, genome sequencing and variant detection

Genomic DNA of inbred MR-VP and each selection and control population was extracted from female mites according to Van Leeuwen et al. (Van Leeuwen et al., 2008). Briefly, 4 × 200 adult mites/population were homogenized in a 2 ml Eppendorf tube containing 800 µl of SDS buffer (2% SDS, 200 mM Tris-HCl, 400 mM NaCl, 10 mM EDTA, pH = 8.33), followed by DNA extraction using a previously described phenol-chloroform-based protocol (Van Pottelberge et al., 2009a). Prior to adding isopropanol, the four extracts were pooled and precipitated together to obtain sufficient DNA per population. Subsequently, samples were further column-purified using an EZNA Cycle Pure Kit (Omega Bio-tek, Norcross, GA, USA) according to the manufacturer's protocol and quantified using an ND-1000 NanoDrop spectrophotometer (Thermo Fisher Scientific, Waltham, MA, USA).

Illumina genomic DNA libraries were constructed, and sequencing was performed to generate paired-end reads of 101 bp (inbred MR-VP strain) or 125 bp (all other samples). Library construction and sequencing was performed at either the Centro Nacional de Análisis Genómico (CNAG, Barcelona, Spain) for inbred MR-VP strain or the Huntsman Cancer Institute of the University of Utah (Salt Lake City, UT, USA) (all segregating populations). Genomic sequence reads for strain MR-VP and the segregating populations have been deposited in the Sequence Read Archive under accession numbers SAMN11350708-SAMN11350748. Illumina reads were aligned to the reference Sanger draft *T. urticae* genome from the London strain (Grbić et al., 2011) using the default settings of the Burrows-Wheeler Aligner (BWA) version 0.7.15-r1140 (Li and Durbin, 2009) and processed into position-sorted BAM files using SAMtools 1.3.1 (Li et al., 2009). Following recommendations described in the Genome Analysis Toolkit (GATK) best practices pipeline (Van der Auwera et al., 2013), duplicates were marked using Picard tools 2.6.0 (https://broadinstitute.github.io/picard), followed by indel realignment with GATK version 3.6.0-g89b7209 (McKenna et al., 2010). Joint variant calling across all 40 populations and the parental strains was carried out with GATK's UnifiedGenotyper tool to produce a variant call format (VCF) file containing single nucleotide polymorphisms (SNPs) and indels.

2.7. Quality control on predicted variants

To be informative for downstream genetic analyses, variants needed to segregate (i.e., be fixed for contrasting alleles in the MR-VP and Wasatch inbred parental strains) and be of high quality. SNPs were therefore selected according to the following criteria, which were adapted from the hard-filtering recommendations in GATK post #2806 (https://gatkforums.broadinstitute.org/gatk/discussion/2806/howto-apply-hard-filters-to-a-call-set, accessed 9 July 2018): (1) have a minimum quality score normalized by allele depth (QD; this and subsequent acronyms and abbreviations refer to how the metrics appear in the VCF 4.2 standard) of 2, (2) mean root square mapping quality (MQ) of at least 50, (3) strand odds ratio (SOR) below 3, (4) mapping quality rank sum (MQRankSum) higher than or equal to −8, (5) rank sum for relative positioning of alleles in reads (ReadPosRankSumTest) of at least −8, and (6) be within 25% and 150% of the sample's genome-wide mean SNP read coverage to minimize false heterozygous variant calls caused by copy number variable regions (see also Wybouw et al., 2019); this was calculated using total depth per allele per sample (AD).

2.8. Responses to selection and validation of the T. Urtiace three-chromosome assembly

For most downstream analyses, we transformed variant positions as assessed on the *T. urticae* draft Sanger genome assembly onto the recently reported *T. urticae* three-chromosome assembly (Wybouw et al., 2019). For simplicity, we refer to pseudochromosomes 1–3 in this assembly as chromosomes 1–3 (Chr1-3). This assembly was constructed

with replicated population allele frequency data from 22 populations in an earlier study, and was partially validated with short-read *de novo* assemblies from multiple *T. urticae* strains (Wybouw et al., 2019). The authors of this study noted that additional, dense population allele frequency would be important to validate the assembly. To do this, and to assess the appropriateness of the assembly for use in our study, we calculated the average window distance (AWD) metric across Chr1-3 using the allele frequency data of all of our 39 individual population samples (one of the 40 segregating populations was excluded from the analysis, see Section 2.10). Briefly, as assessed from highly replicated population allele frequency data, positive deflections of the AWD metric by position in genome-wide scans detect assembly errors; our implementation of AWD calculations followed that of Wybouw et al. (2019).

2.9. Heterozygosity estimates

To verify that strains MR-VP and Wasatch were inbred to fixation, we used a separate joint variant call analysis to estimate genome-wide levels of heterozygosity. Briefly, to improve variant call accuracy, and to provide an expectation for inbreeding to homozygosity, we included, in addition to MR-VP and Wasatch, previously published inbred and non-inbred sequenced strains of *T. urticae*: Albino-JP, Foothills, Lon-Inb, MAR-AB, PA2, and SR-VP (Bryon et al., 2017; Wybouw et al., 2019). The predicted variants were filtered as described above, with modifications and additional filtering steps to reduce the number of false positives. Specifically, MQRankSum and ReadPosRankSumTest filters were bidirectional, meaning we kept alleles that fell between −8 and 8 for both. In addition, to prevent copy number variable regions from falsely elevating the heterozygosity estimates, only alleles falling within 25% of the mean genome-wide SNP coverage depth for each strain were considered. The extent of heterozygosity, as assessed from counts for alleles at high-quality SNP positions in sliding windows, was visualized genome-wide.

2.10. Principle component analysis

A principal component analysis (PCA) was performed in R version 3.4.3 (R Developement Core Team, 2015). A correlation matrix containing the individual SNP frequencies for specific alleles was used as input for the R function prcomp, which is part of the R package 'stats' (version 3.3.0). We selected only those SNP alleles that were present in all treatments (fenpyroximate-selected, pyridaben-selected, tebufenpyrad-selected and control). The PCA plots were created with autoplot, a function of the R package 'ggplot2' (version 2.1.0) (Wickham, 2009). An examination of the resulting PCA analysis identified an extreme outlier in the pyridaben-selected group (Fig. S1), presumably reflecting contamination by an unrelated strain; this sample, P9, was therefore excluded from all subsequent analyses, and a PCA with all samples except P9 was then generated.

2.11. Bulked segregant analysis genetic mapping

The ~590,400 loci from strains MR-VP and Wasatch were analyzed using BSA methods adapted from earlier studies (Bryon et al., 2017; Demaeght et al., 2014; Van Leeuwen et al., 2012; Wybouw et al., 2019). The difference in MR-VP allele frequency between the acaricide-selected and the control samples was averaged for each pesticide treatment in overlapping 75 kb genomic windows with 5 kb offsets. Statistical significance of BSA peaks, as assessed across all replicates, was determined with the permutation approach of Wybouw et al. (2019). Briefly, in replicated BSA data, responses to selection among independent replicates are expected to co-occur at the same genomic locations. Alternatively, where minor peaks are solely due to drift, no systematic co-occurrence between replicates is expected. The permutation method implemented by Wybouw et al. (2019) assigns genomic regions responding to selection across samples (concerted responses at specific genomic locations) from multigenerational, replicated unselected and selected populations by establishing a significance threshold for QTL detection at a specified genome-wide false discovery rate (FDR). The permutation method requires pairing of selected and unselected samples. In this study, we adapted the sample matching approach that Wybouw et al. (2019) applied to the same experimental design to detect a QTL for host plant adaptation using five selected and unselected populations. An exception was that, as the current study used many more replicates – 9 for pyridaben and 10 for fenpyroximate and tebufenpyrad (hence 9! and 10! potential pairings) – subsets of 120 potential pairings were chosen to make it computationally feasible. For each of the 120 sets, 5% FDR thresholds for QTL detection were calculated from the distribution of maximal allele frequency values for 10^4 permutations as described by Wybouw et al. (2019). Across the entire set of 120 permutations, the most conservative 5% FDR cutoff was used for QTL assignment.

2.12. Predicted effects of genetic variants in coding sequences

To assess coding sequence changes in genomic (QTL) regions for response to pesticide selection, coding effects of SNPs and small indels identified by the GATK analysis were predicted using SnpEff 4.2 (Cingolani et al., 2012) with a *T. urticae* coding sequence database derived from the June 23, 2016 annotation available from the Online Resource for Community Annotation of Eukaryotes (ORCAE) (Sterck et al., 2012). The QTL were also visually inspected in Integrative Genomics Viewer (IGV) version 2.3.90 (Robinson et al., 2011).

2.13. Alignment of CPR proteins

All protein sequences used in the alignment were accessed either using the UniProt database (Bateman et al., 2015): (*T. urticae* (tetur18g03390), *H. sapiens* (NP_000932.3), *R. norvegicus* (NP_113764.1), *M. domestica* (NP_001273818.1) and *D. melanogaster* (NP_477158.1) or NCBI: *C. sculpturatus* (XP_023225549.1). The sequences were aligned using Clustal W version 2.1 (Larkin et al., 2007).

2.14. Gene duplication of the DNA-binding domain (DBD)-lacking nuclear hormone receptor (NHR-96)-like gene within a QTL connected with tebufenpyrad selection

De novo assemblies of inbred strains MR-VP and Wasatch were constructed from paired-end Illumina data using CLC Genomics Workbench 9.0.1 (https://www.qiagenbioinformatics.com). Reads were imported and trimmed using the "Trim Sequences" tool prior to assembly with the "De Novo Assembly" tool; default settings were used for both. Contigs from the *de novo* assemblies were aligned to the London reference genome using the default settings of BLASR 1.3.1 (Chaisson and Tesler, 2012) with soft-clipping enabled. Contig sequences aligning to the DBD-lacking NHR 96-like gene in the QTL region for response to tebufenpyrad (*tetur06g04270*) were extracted (File S1) and their open reading frames (ORFs) determined using ExPASy (Gasteiger et al., 2003). RNA-seq alignments were performed using Spliced Transcripts Alignment to a Reference (STAR) version 2.5.3a (Dobin et al., 2013), with the two-pass mode and a maximum intron size of 20 kb; the RNA-seq reads were aligned to a modified version of the London reference sequence that was adjusted to include an MR-VP *de novo* assembled contig in the genomic region spanning *tetur06g04270*. Gene duplications in both Wasatch and MR-VP *de novo* contigs were annotated (File S2) based on the ORF information and the MR-VP RNA-seq alignment visualization in IGV version 2.3.90 (Robinson et al., 2011).

Table 1
Results of toxicity bioassays for the inbred parental strains MR-VP and Wasatch. Strain MR-VP showed significantly higher levels of resistance compared to strain Wasatch for every acaricide tested. METI-I resistance of MR-VP had also been determined prior to the strain's inbreeding by Van Pottelberge et al. (2009b).

	Inbred Wasatch LC50 (mg a.i. L^{-1}, 95% CI)	Inbred MR-VP LC50 (mg a.i. L^{-1}, 95% CI)	Resistance factor	MR-VP before inbreeding LC50 (mg a.i. L^{-1}, 95% CI)
Fenpyroximate	26.357 (18.161–32.101)	> 5000	> 190	10581 (8441–13036)
Pyridaben	4.274 (3.759–4.845)	2275.72 (1944.83–2663.03)	532	36959 (26450–59590)
Tebufenpyrad	5.722 (4.788–6.818)	416.932 (356.990–475.636)	73	1197 (1080–1309)

2.15. Analysis of DBD-lacking NHR96-like genes in T. urticae: manual reannotation, phylogeny, and genomic distribution

The *T. urticae* genome was mined for other DBD-lacking NHR96-like genes by using the eight conserved NHR96-like ligand binding domains (LBDs) as queries in tBLASTn and BLASTp searches (e-value threshold of e^{-3}, BLAST+ version 2.2.31) against the *T. urticae* genome (Grbić et al., 2011) and proteome (version of 11 August, 2016), respectively. *T. urticae* gene models were modified when necessary or new gene models were created using GenomeView version N39 (Abeel et al., 2012). The DBD-lacking NHR96-like sequences can be found in File S3. To test for evidence of other tandem duplications of DBD-lacking *T. urticae* NHR-like genes, Chr1-3 and the smaller unplaced scaffolds were scanned for regions where at least two DBD-lacking NHR genes occurred in the same orientation with 50 kb or less between each pair of genes within the cluster.

Subsequently, nuclear receptor sequences were obtained for *Drosophila melanogaster*, *Daphnia pulex* and *T. urticae* (Grbić et al., 2011; King-Jones and Thummel, 2005; Thomson et al., 2009) [accession numbers can be found in Table S1]. Using Pfam 31.0 (Finn et al., 2016), each receptor sequence was analyzed for the presence of a conserved LBD (PF00104). Detected LBDs were aligned to those of the mined candidate *T. urticae* DBD-lacking NHR96-like peptides using MAFFT version 7 with the E-INS-i iterative refinement method strategy (Katoh et al., 2002). A phylogenetic analysis was performed on the CIPRES web portal (Miller et al., 2010) using RAxML version 8 HPC2-XSEDE (Stamatakis, 2014) with the automatic protein model assignment algorithm using the maximum likelihood criterion and 1000 bootstrap replicates; the LG + G protein model was selected as the optimal model for analysis. The resulting tree was midpoint rooted, visualized using MEGA6 (Tamura et al., 2013) and edited in CorelDRAW Home & Student X7 (Corel, Austin, TX, USA).

2.16. NHR-like genes lacking DBD in other arthropods

To determine if DBD-lacking NHR genes (including DBD-lacking NHR96-like genes) were common in other arthropods, we used two approaches: one relying on comprehensive searches of the NCBI nr database (downloaded 13 June, 2018) for DBD-lacking NHR-like genes using keywords, and the other based on BLASTp (version 2.7.1) searches with DBD-lacking NHR96-like *T. urticae* gene queries against the same database; the latter approach was undertaken to find NHR-like genes that had not been annotated. Using the first approach, we extracted all protein sequences that had "nuclear receptor", "hormone receptor", or "ecdysone" in their description; the last keyword was used as many insect NHRs are involved in molting and metamorphosis (Fahrbach et al., 2012). For the second approach, we used as queries each of the 47 DBD-lacking NHR96-like genes present in the London genome sequence of *T. urticae*, as well as the two copies of the *tetur06g04270* gene from strain Wasatch. We allowed 1000 results for each search and then extracted all the resulting proteins that aligned with an e-value of 1 or below.

From the protein sequences obtained using both approaches, we only kept those belonging to Arthropoda as assessed with the Python package ete3 (version 3.1.1) (Huerta-Cepas et al., 2016). InterProScan version 5.29–68.0 was then used to predict domains and conserved regions. From the resulting sequences, we extracted those that were classified by InterProScan as "nuclear hormone receptor-like domain superfamily" (IPR035500), and that lacked the "Zinc-finger, nuclear hormone receptor type" motif (IPR001628) (Zdobnov and Apweiler, 2001). In the event that several proteins had the same amino acid sequence, only one was retained for analysis.

3. Results

3.1. Characterization of METI-I resistant inbred strains

To facilitate genetic and genomic analyses, strain MR-VP was mother-son inbred for six generations, a level of inbreeding similar to that of strain Wasatch, which was performed in an earlier study (Bryon et al., 2017). To confirm that the strains were isogenic, we sequenced the MR-VP strain using the Illumina method, and aligned the resulting reads, as well as those from Wasatch and several other strains sequenced previously (Bryon et al., 2017), to the London reference genome. For strains like MAR-AB and Albino-JP, which were either not inbred, or only inbred for one generation (Bryon et al., 2017), heterozygosity was observed at 82.14% and 10.29% of SNP sites, respectively. In contrast, for MR-VP and Wasatch, only 1.77% and 1.14% of variable positions were not fixed (Fig. S2), respectively, perhaps reflecting sequencing errors or errant predictions in copy number variable regions. Toxicity bioassays revealed that the inbred MR-VP and Wasatch strains varied greatly in their susceptibility to METI-Is, with MR-VP withstanding 190-, 532- and 73-fold higher concentrations of fenpyroximate, pyridaben and tebufenpyrad, respectively (Table 1). In fact, MR-VP's LC_{50} for fenpyroximate could not be calculated as it exceeded 5000 mg a.i. L^{-1}.

3.2. Evolution of METI-I acaricide resistance in experimental mite populations

To establish a segregating population for genetic mapping of resistance, we crossed MR-VP to Wasatch, and then crossed the F_1 hybrid population back to Wasatch. This backcross was performed to maximize the recombination of haplotypes contributed by the resistant MR-VP strain. After the resulting population was allowed to expand in bulk for several generations, ten subpopulations were established for each of the three acaricide treatments, in addition to ten control subpopulations (see Materials and Methods). The 40 resulting populations were reared in separation in a greenhouse on whole bean plants for over nine months (~25 generations). During that time, each population in the three treatment groups was adapted to gradually increasing concentrations of acaricide, ending with the final concentrations of 3500 mg a.i. L^{-1} fenpyroximate, 1250 mg a.i. L^{-1} pyridaben, and 750 mg a.i. L^{-1} tebufenpyrad. Afterwards, the selected and the control populations were tested at 2500 mg a.i. L^{-1} of each acaricide, which proved to be a discriminating concentration that showed a clear distinction between resistant and sensitive populations (Fig. 1). All three acaricide-selected population groups showed significantly higher survival rates compared to the control populations ($p < 0.0001$, generalized mixed model).

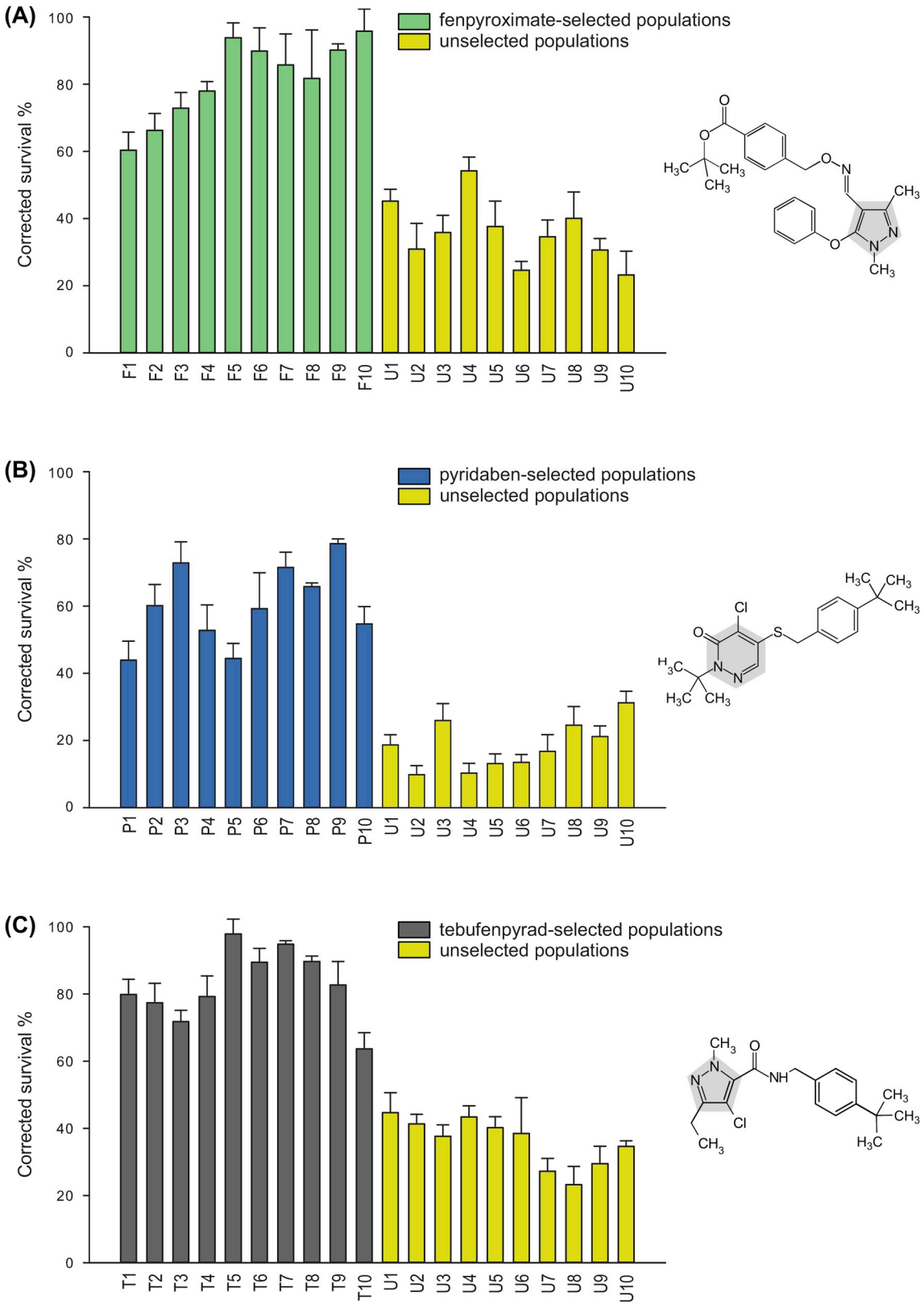

Fig. 1. Response to acaricide treatment for MR-VP × Wasatch recombinant long-term acaricide-selected and control populations. Survival was scored in the adult stage after spraying with 2500 mg a.i. L^{-1} of (A) fenpyroximate, (B) pyridaben and (C) tebufenpyrad. All three sets of acaricide-selected populations showed significantly higher survival rates compared to the control populations ($p < 0.0001$, generalized mixed model). Error bars represent 2 × SE. The molecular structures of the three acaricides are displayed to the right of the bar plots, with nitrogen heterocycles shaded in gray.

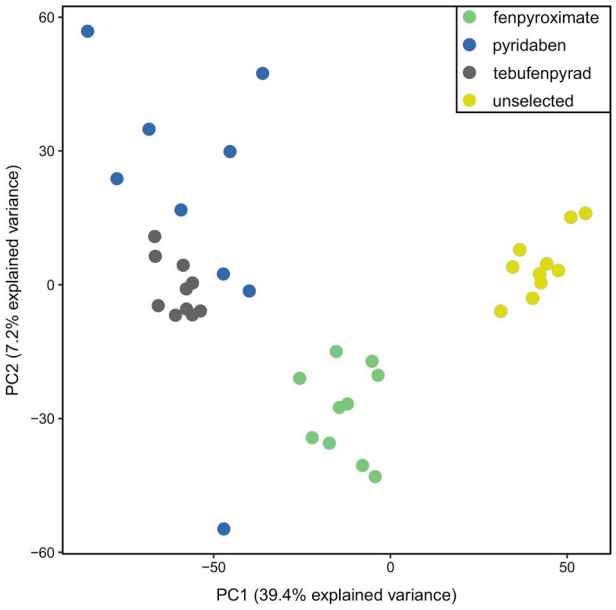

Fig. 2. Principal component analysis (PCA) with control and selected populations based on genome-wide allele frequencies at polymorphic sites. Individual populations are colored according to the treatment group (legend, upper right). The control, fenpyroximate-selected and tebufenpyrad-selected populations clustered tightly by treatment group, and separately from each other. The pyridaben-selected populations clustered less tightly, but nevertheless remained separate from control populations along PC1.

3.3. Genomic responses to selection

Following the experimental selections, we extracted DNA from each of the 40 populations and performed genome sequencing to produce a per-sample Illumina read coverage ranging from 58 to 78 (based on the Variant Call Format [VCF] file; see Materials and Methods). As revealed from alignments of the resulting reads, and those of the MR-VP and Wasatch parents, to the *T. urticae* reference genome (London strain, Grbić et al., 2011), ~590,400 high-quality SNP variants were identified as segregating in the experimental populations. To test for responses to selection, we performed PCAs using the genome-wide variant predictions (Fig. 2). As a preliminary PCA revealed that one pyridaben population was contaminated by an unknown strain (Fig. S1), the analysis was repeated excluding that sample. For the control, fenpyroximate-selected and tebufenpyrad-selected populations, tight clustering was apparent, with no overlap among populations by treatment. Along PC1, which explained 39.4% of the variation, pyridaben- and tebufenpyrad-selected populations clustered separately from control and fenpyroximate-selected populations. However, along PC2 (7.2% of the variation), pyridaben-selected populations were markedly more dispersed as compared to the other treatment groups, consistent with a more heterogeneous response to selection by pyridaben as opposed to the other two acaricides.

3.4. Regional genomic responses to selection and validation of the three-chromosome assembly

As the principle component analysis (PCA) was consistent with genome-wide responses to selection by each acaricide, we assessed the frequency of the MR-VP alleles in sliding windows along Chr1-3 in the consolidated genome assembly recently reported by Wybouw et al. (2019). For the control, fenpyroximate and tebufenpyrad treatments, allele frequencies for populations within treatment groups were highly correlated, as they were between treatment groups over much of the genome length. For the pyridaben populations, greater variation was observed, consistent with the findings of the PCA. A potential explanation for this result is that the pyridaben populations went through a more severe bottleneck during acaricide selection as compared to the selections with the other two compounds (during a bottleneck event, the effect of genetic drift is elevated). Nevertheless, systematic differences were observed in allele frequencies between the control populations and those in each acaricide treatment group (e.g., at ~30 Mb on Chr1), identifying putative regions for adaptation. Using the population allele frequency data from the control and the fenpyroximate-selected, pyridaben-selected and tebufenpyrad-selected populations, we also calculated the average window distance (AWD) metric along the lengths of Chr1-3 (Fig. S3); positive deflections in this metric are indicative of assembly errors, see Wybouw et al. (2019) and Materials and Methods. As no such errors were apparent (confirming the integrity of the three-chromosome assembly), we used this chromosome-level assembly for all further analyses.

3.5. Population bulked segregant analysis mapping of QTL

To detect genomic intervals that responded to acaricide selections, we tested for significant deviations in allele frequencies between fenpyroximate, pyridaben and tebufenpyrad treated populations as compared to the control populations. Using a permutation-based framework for establishing QTL significance that takes into account all replicate data (see Materials and Methods) adapted from Wybouw et al. (2019), we identified one or more QTL for resistance for each of the three acaricides at a FDR of 5% (Fig. 3). Within an acaricide-control comparison, QTL were prefixed with the acaricide, and numbered in order from strongest to weakest as assessed by the magnitude of the allele frequency deviations. In all cases, significant QTL reflected selection for alleles contributed by the resistant MR-VP parent. For each QTL region, we analyzed genes and genetic variants in the top 75 kb window as assessed from the BSA genomic scans.

All three acaricide-selected groups shared a QTL at a coincident location at ~30 Mb on Chr1 (fenpyroximate-, pyridaben- and tebufenpyrad-QTL 1; Fig. 3A–C, respectively). Strikingly, in all the METI-I-selected populations, the haplotype contributed by the resistant MR-VP strain went to complete (or nearly complete) fixation (Fig. S3A–C). The top windows for each of these three QTL all harbored NADH: ubiquinone oxidoreductase (also known as PSST, *tetur07g05240*), and the putative H92R target-site resistance allele for fenpyroximate, pyridaben, and tebufenpyrad (Bajda et al., 2017), among a total of 21 genes in the collective region of 80 kb spanning the three peak windows of response (Fig. 4; Table S2).

In addition, for the pyridaben and tebufenpyrad selections, a QTL for resistance was also observed at a coincident location on Chr2 (at ~5.7 Mb, pyridaben- and tebufenpyrad-QTL 2; Fig. 3B and C, respectively). The top 75 kb peak genomic windows overlapped exactly for these two QTL, and the region harbored 27 annotated genes (Table S3). Within this region, cytochrome P450 reductase (CPR, *tetur18g03390*), which encodes an enzyme required for P450 function (Demaeght et al., 2013; Riga et al., 2015), was located within 20 kb of the maximal allele frequency deviations (Fig. 4B). An analysis of the MR-VP haplotype revealed that it was identical to that of the spirodiclofen-resistant strain SR-VP studied by Wybouw et al. (2019); in this study, the authors identified a nonsynonymous variant, D384Y, as unique to SR-VP and only one other strain published to date. While this variant was also present in MR-VP, it was absent in the METI-I sensitive parent, Wasatch.

A QTL at ~12.5 Mb on Chr1 was specific for the tebufenpyrad group (tebufenpyrad-QTL 3, Fig. 3C; while pyridaben-selected populations also showed elevated MR-VP allele frequencies in this region, they did not pass the significance threshold). The top window for response to tebufenpyrad selection was located near a DNA-binding domain (DBD)-lacking nuclear hormone receptor 96 (NHR96)-like gene (*tetur06g04270*), among a total of 15 genes (Table S4).

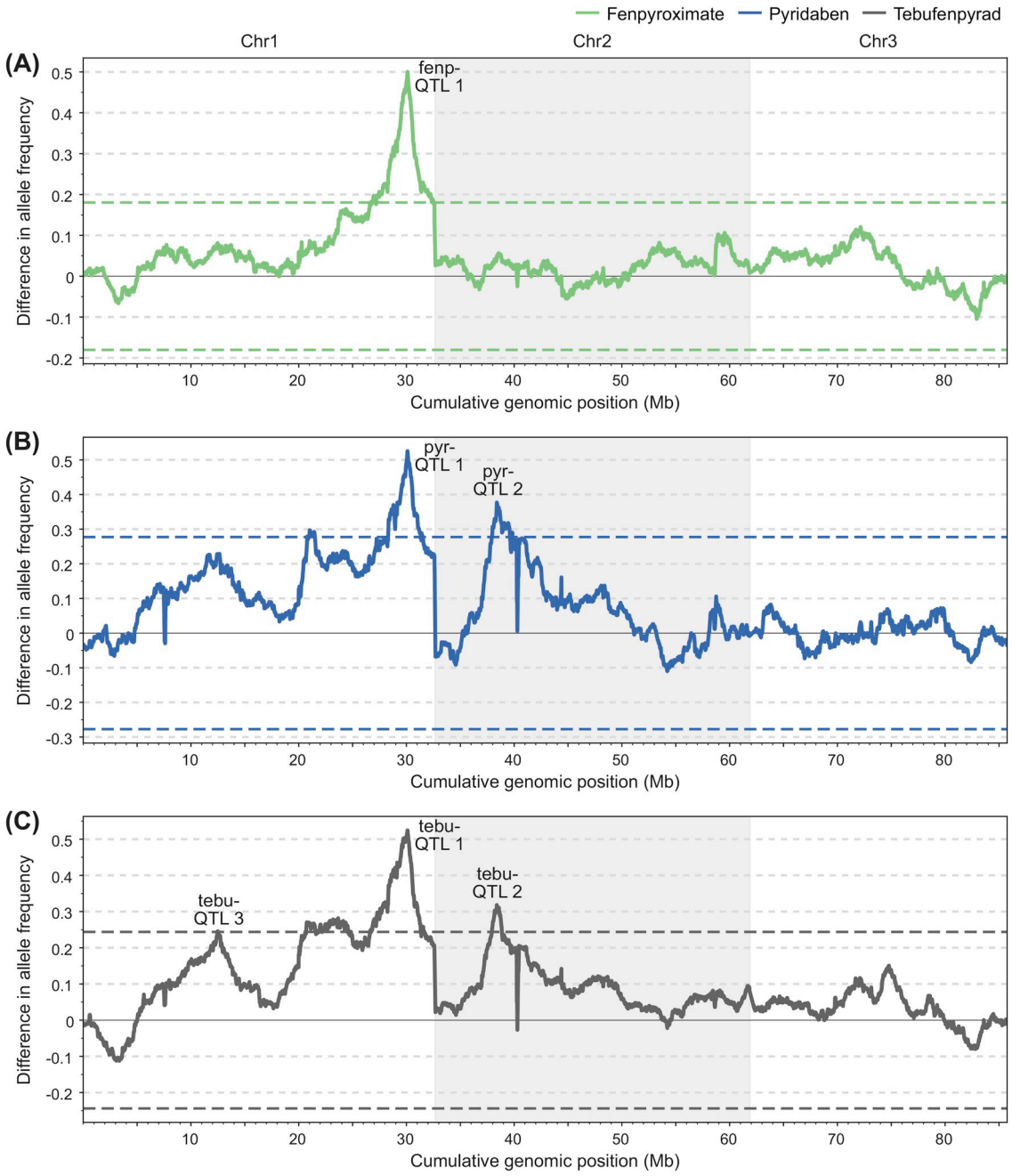

Fig. 3. Genomic responses to acaricide selections. Bulked segregant analysis (BSA) genetic mapping of QTL for resistance to (A) fenpyroximate (green), (B) pyridaben (blue), and (C) tebufenpyrad (gray). Dashed lines delineate statistical significance for QTL detection (FDR of 5%). A QTL at a coincident location at ~30 Mb on Chr1 (QTL 1) was observed for selection by each acaricide, and corresponds to the target-site H92R mutation in NADH: ubiquinone oxidoreductase (PSST). Coincident BSA peaks centered on cytochrome P450-reductase (CPR) on Chr2 (QTL 2) and were observed in response to selection by both pyridaben and tebufenpyrad. A less dramatic but nonetheless significant BSA peak at ~12.5 Mb on Chr1 (QTL 3) was only observed in response to selection by tebufenpyrad, and is located nearby two tandemly duplicated nuclear hormone receptor 96 (NHR96)-like genes that lack the DNA-binding domains (DBDs). (For interpretation of the references to color in this figure legend, the reader is referred to the Web version of this article.)

In addition, we noted that the pyridaben- and tebufenpyrad-selected populations had elevated frequencies of MR-VP alleles, relative to the control populations, over a broad region from about 20 to 25 Mb on Chr1. Although portions of this large interval passed the threshold for QTL detection, the region is located along the proximal slope of the large response region for pyridaben- and tebufenpyrad-QTL 1. Whether this region reflects one or more independent QTL, or rather the physical proximity to QTL 1 (hitchhiking due to linkage), will require additional investigation.

3.6. Analysis of D384Y mutation in CPR

The D384Y change in the CPR gene of MR-VP was first reported in a genomic region that showed significant response to spirodiclofen selection in *T. urticae* strain SR-VP (Wybouw et al., 2019). The CPR gene is highly conserved in all organisms and therefore alignments and modeling on known CPR structures are straightforward. Fig. 5 shows an alignment of the *T. urticae* CPR sequence with other animal CPRs in the region surrounding D384. When modeling CPR with Phyre2 (Kelley et al., 2015), an excellent match with rat CPR (pdb: c1j9zB) was

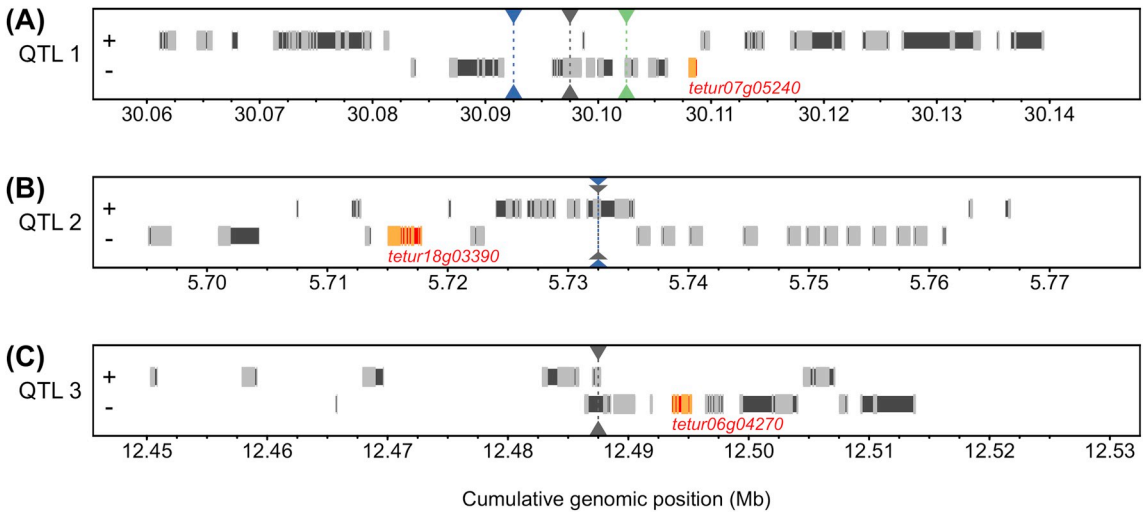

Fig. 4. Genes in 75 kb genomic windows of peak response at QTLs 1–3. Triangles positioned along the top and bottom boundaries of each plot represent genomic window midpoints of each acaricide treatment group: fenpyroximate-selected (green), pyridaben-selected (blue), and tebufenpyrad-selected (gray). The orientation of gene models is as indicated ("+" or "-" for forward and reverse strands, respectively). Coding exons are denoted by rectangles shaded in light gray, and introns are shaded in darker gray. Putative candidate genes at the BSA peaks are highlighted in orange (the June 2016 *T. urticae* annotation, Online Resource for Community Annotation of Eukaryotes, or ORCAE, was used). The candidate genes are: (A) QTL 1 (all selections); target enzyme NADH: ubiquinone oxidoreductase (PSST; *tetur07g05240*), (B) QTL 2 (pyridaben and tebufenpyrad selections); cytochrome P450 reductase (CPR) (*tetur18g03390*), and (C) QTL 3 (tebufenpyrad selections only); nuclear hormone receptor 96 (NHR96)-like DNA-binding domain (DBD)-lacking (*tetu06g04270*). (For interpretation of the references to color in this figure legend, the reader is referred to the Web version of this article.)

obtained (score of 1184.13, e-value = 0, probability 100% with 58% identities). Spider mite D384, which corresponds to rat or human Q391, was located on the surface of the protein, specifically at the end of alpha helix I (nomenclature of Wang and Roberts, 1997) in the connecting domain between the conserved FAD/NADPH and FMN domains. This region is not implicated in flavin cofactor or NADP(H) binding, and is distant from the short "hinge" connecting the two flavin domains of CPR. Hence, the mutation was not predicted to interfere in any major and obvious way with electron transfer from NADPH to FAD and FMN, or electron transfer between the reductase and P450, but it may have more subtle effects (see Discussion).

3.7. Nuclear hormone receptor analysis

We identified a DBD-lacking NHR96-like gene (*tetur06g04270*) as one of the candidate genes potentially linked with tebufenpyrad resistance. Aligning *de novo* assembled contigs to the three-chromosome assembly suggested that *T. urticae* strains MR-VP and Wasatch both harbored two copies of the DBD-lacking NHR96-like gene in tandem in a head-to-tail orientation. Next, to verify gene models and to determine if the genes were expressed, we aligned MR-VP RNA-seq reads to a copy of the three-chromosome assembly in which a *de novo* assembled MR-VP contig spanned the *tetur06g04270* region in place of the original sequence. As the RNA reads uniquely mapped to each gene, the alignments confirmed the presence of the duplication and showed that both genes were expressed in MR-VP (Fig. S4).

The NR1J group represented in insects by the single NHR96 receptor was shown to be expanded in *T. urticae*, where eight NHR96-like genes were found (Grbić et al., 2011). However, all of them contained the DBD. In this study, we annotated DBD-lacking NHR96-like genes in the *T. urticae* genome and identified 47 genes that had a ligand-binding domain (LBD) most similar to the eight canonical NHR96-like genes previously reported (Cheng et al., 2008; Grbić et al., 2011; Robinson-Rechavi et al., 2003; Thomson et al., 2009), but that lacked the DBD (Fig. 6, panel A). Most DBD-lacking NHR96-like genes in *T. urticae* (37/47) occurred in clusters (i.e., within 50 kb of another DBD-lacking NHR-gene in a head-to-tail orientation) of up to seven genes, suggesting sequential duplication events (Fig. 6B).

To determine if DBD-lacking NHR-like (and specifically, NHR96-like) peptides were common in other arthropods, we comprehensively searched the NCBI database for NHR-like DBD-lacking proteins. By far the most common types of previously annotated DBD-lacking NHR-like receptors were E75s (88 in total), followed by FTZ-F1s (44), E78s (41), and photoreceptors (20). DBD-lacking NHR96-like genes, on other hand, appeared to be relatively rare. Our nr database search only identified a single annotated DBD-lacking NHR96 peptide in each of the following species: *Agrilus planipennis*, *Centruroides sculpturatus*, *Drosophila miranda*, *Plutella xylostella*, and *Rhagoletis zephyria*.

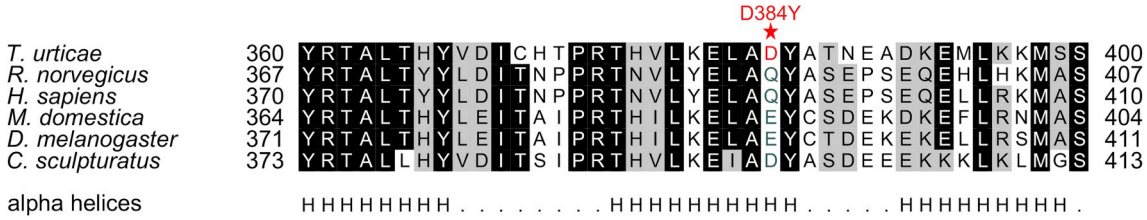

Fig. 5. Alignment of cytochrome P450 reductase (CPR) sequences around the D384Y variant. The conservation of alpha helices H (left), I (middle) and J (right) is shown. An 80% threshold was used for identity (black background) and similarity shading (gray background). The D384Y variant is located at the end of helix I (red star). The residue is charged in arthropods (D in the scorpion *C. sculpturatus* and the spider mite and E in the insects *M. domestica* and *D. melanogaster*), while most vertebrates have a polar Q at that position. The homologous Q391 in the human CPR is predicted to interact with the FMN domain in the open conformation in which electron transfer to P450s occurs. (For interpretation of the references to color in this figure legend, the reader is referred to the Web version of this article.)

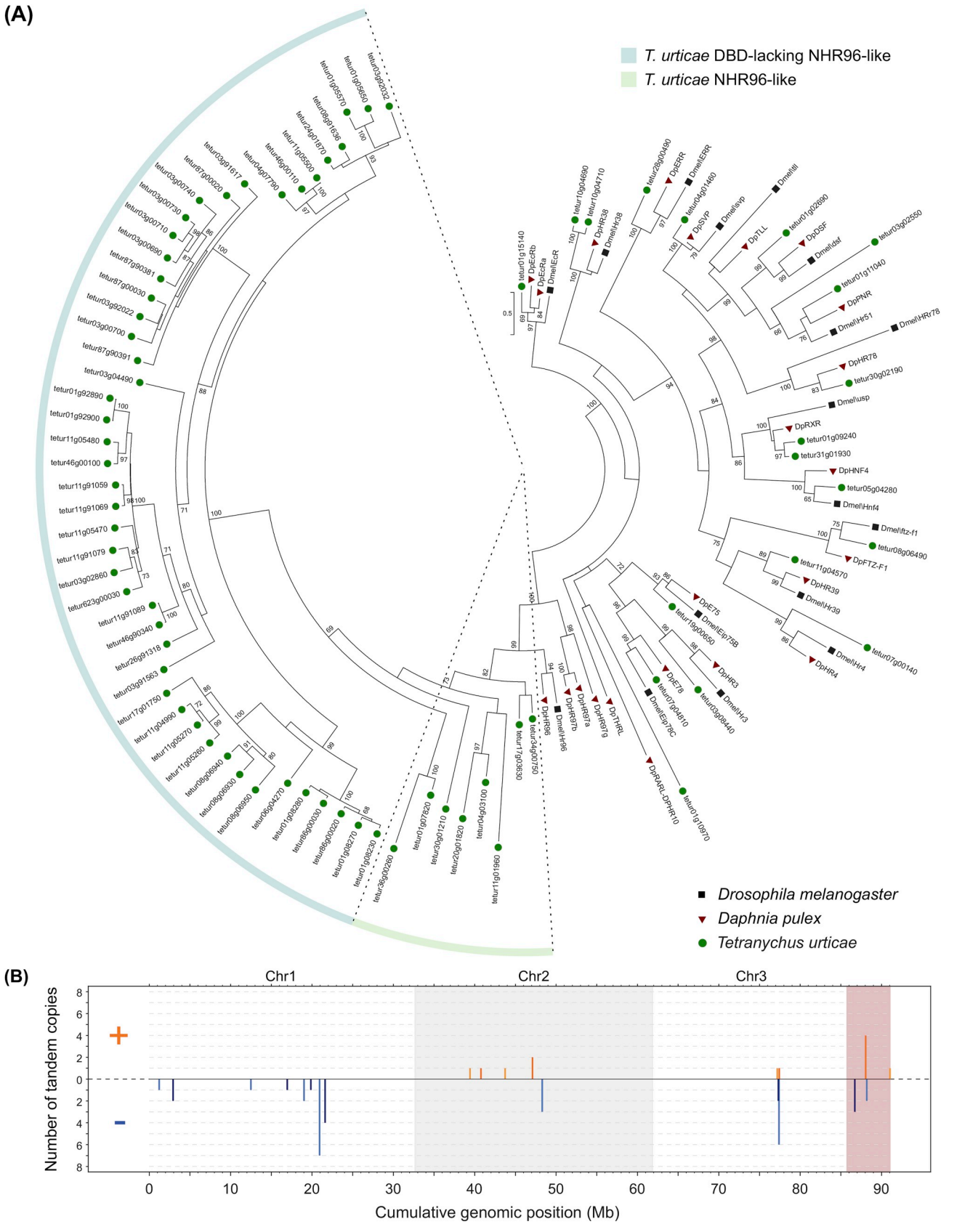

(caption on next page)

Fig. 6. Phylogenetic analysis of *T. urticae* nuclear hormone receptor (NHR) genes, and genomic distribution of *T. urticae* DNA-binding domain (DBD)-lacking NHR96-like genes. (A) Maximum likelihood LG + G phylogenetic tree of NHRs in *D. melanogaster*, *D. pulex* and *T. urticae*. Only bootstrapping values higher than 65 are shown. The scale bar represents 0.5 amino acid substitutions per site. Both *T. urticae*-specific DBD-lacking NHR96-like and canonical NHR96-like gene expansions are shaded. (B) Genomic distribution of *T. urticae*'s DBD-lacking NHR96-like genes is shown with lengths of vertical line segments corresponding to the number of genes clustered (i.e., within 50 kb of another such gene) in a head-to-tail orientation. The orientation was delineated by "+" and "-" along the y-axis and by plotting the bars in shades of orange and blue, respectively. Only intact DBD-lacking NHR96-like genes were included in the analysis. The chromosomes are indicated by alternating white and gray shading, while small scaffolds were concatenated and shaded in red to the right of the chromosomes. (For interpretation of the references to color in this figure legend, the reader is referred to the Web version of this article.)

4. Discussion

Previous investigations into METI-I resistance in MR-VP revealed that fenpyroximate and pyridaben resistance were inherited as a monogenic and dominant trait, whereas resistance to tebufenpyrad was polygenic and incompletely dominant (Van Pottelberge et al., 2009b). Subsequently, sequencing of several subunits presumably making up the target/binding-site identified a nonsynonymous H92R change in the PSST subunit of NADH:ubiquinone oxidoreductase, which was significantly associated with resistance (Bajda et al., 2017). Nevertheless, the introgression of this mutation into a susceptible genetic background revealed that the H92R variant alone failed to explain the strength of the resistance phenotype to any of the three acaricides. This suggested roles for other loci and alleles in resistance.

In this study, we subjected a segregating population (parental strains MR-VP and Wasatch, which are resistant and sensitive, respectively) to multiple rounds of selection by three METI-Is, and used BSA genetic mapping to identify loci responding to selection for each acaricide. While the H92R change played a significant role in resistance to each acaricide, one additional genomic region was significantly associated with resistance to both pyridaben and tebufenpyrad, and a further QTL was identified for tebufenpyrad resistance alone. The peak regions of response for both additional QTL harbored candidate genes encoding an enzyme or putative receptors associated directly or indirectly with xenobiotic detoxification (CPR, and two tandem NHR96-like genes lacking DBDs). The candidate genes, and in some cases putative variants for QTL, are discussed below, although for CPR and the NHR96-like genes our conclusions are speculative.

The target-site H92R variant in the PSST subunit was coincident with the most prominent peak in all three BSA scans (QTL 1). The unselected populations were relatively resistant compared to the susceptible parent (Fig. 2), presumably reflecting the high frequency of the H92R variant in the unselected populations – about 0.5 after ~25 generations in the experimental evolution experiment (Fig. S3) – likely reflecting the partially dominant nature of the change (Van Pottelberge et al., 2009b). This pattern reveals that contrary to the fitness cost associated with some resistance mutations in *T. urticae* (Riga et al., 2017) and the lethality of the corresponding substitution in *Drosophila melanogaster* (Bajda et al., 2017), there is no major fitness cost associated with the *T. urticae* H92R substitution. The earlier work, as well as our current study, suggest that mutations occurring in this conserved part of the PSST subunit can have species-specific effects on fitness. Further, mutations in the adjacent PSST subunit residue M91 in the aerobic yeast *Yarrowia lipolytica* decreased enzymatic activity of complex I (Fendel, 2008), but had no effect on V_{max} when binding ubiquinone-1 and even increased V_{max} involving ubiquinone-2, which has a longer isoprenoid side chain (Angerer et al., 2012; Fendel et al., 2008).

In addition to the target-site change, mites selected to pyridaben and tebufenpyrad showed significant responses in other genomic regions. This was consistent with the previously reported incompletely dominant inheritance of tebufenpyrad resistance, but contradicted an earlier result, which classified resistance to pyridaben as monogenic (Van Pottelberge et al., 2009b). The likely explanation is that Van Pottelberge and colleagues used a fairly recently collected outbred MR-VP strain, while we used an inbred derivative of the same strain after it had been maintained in the lab for ~11 years under constant selection (minor effect alleles may have been selected in the laboratory as acaricide concentrations become high enough to overcome target-site resistance).

Introgression of the H92R resistant allele into a sensitive background only resulted in a fraction (average of 578 mg L^{-1} (Bajda et al., 2017)) of the MR-VP fenpyroximate resistance phenotype observed in both this study (> 5000 mg L^{-1}) and in Van Pottelberge et al. (10,581 mg L^{-1}). Nevertheless, fenpyroximate resistance appeared to be monogenic in both Van Pottelberge et al. as well as in our study. While most of the resistance phenotype was likely due to multiple alleles of minor effect that could not be detected by our methods, it remains unknown why neither of the two genomic regions associated with selection to the other acaricides showed a significant association with fenpyroximate resistance. Evidence from functional cytochrome P450 expression in *E. coli* as well as from the application of a selective P450-inhibiting synergist piperonyl butoxide (PBO) suggests that fenpyroximate's metabolism is different from that of pyridaben and tebufenpyrad (see below). The divergent genomic response to selection could thus be related to metabolic resistance, and specifically, to differences in P450-mediated detoxification.

The second most prominent BSA peak (QTL 2) in the tebufenpyrad- and pyridaben-selected *T. urticae* centered on a D384Y mutation in the electron transfer flavoprotein CPR (Wybouw et al., 2019). CPR is an essential enzyme in all eukaryotes that serves as an electron donor protein for all microsomal P450s and several other enzymes found in the endoplasmic reticulum of most cells (Murataliev et al., 2004). CPR was not differentially expressed in MR-VP compared to the METI-I susceptible strain London (Dermauw et al., 2013). Therefore, the D384Y mutation likely does not affect the expression of CPR. Instead, it is possible that the mutation is advantageous by improving P450 detoxification pathways.

The idea that a mutation in CPR can be implicated in resistance development by interacting with relevant P450s in *trans* is attractive, because detoxification of METI-Is is thought to be mostly P450-based (Cho et al., 1995; Devine et al., 2001; Herron and Rophail, 1998; Ozawa, 1994; Van Pottelberge et al., 2009b). This, however, raises the question of why selection to fenpyroximate did not favor the mutation. Possible explanations include the relative specificity of P450s that metabolize acaricides as well as the relative specificity in the interactions of CPR with P450s. P450 specificity towards acaricides is supported by evidence that certain P450s target fenpyroximate, but do not act on the other two acaricides; CYP392A11, a P450 that is overexpressed in MR-VP compared to the METI-I sensitive strain London (Dermauw et al., 2013), hydrolyzes fenpyroximate but not pyridaben or tebufenpyrad when expressed in *E. coli* (Riga et al., 2015). Evidence that other P450s may also fall into this pattern comes from treatment with the synergist PBO, which does not suppress every P450 equally (Feyereisen, 2015). Work on strain MR-VP prior to inbreeding showed that PBO significantly decreased resistance to pyridaben and tebufenpyrad, but had little effect on fenpyroximate resistance (Van Pottelberge et al., 2009b), likely because PBO did not sufficiently target P450s that metabolize fenpyroximate. Specificity in the interactions of CPR with P450s is supported by evidence that human variants in CPR differentially affect various P450 activities (Burkhard et al., 2017). The only known human CPR variant with increased activity is Q153R, and the effect of this mutation is positive on CYP19A1 and CYP3A4

activities but negative on CYP17A1 and CYP51A1 (Udhane et al., 2017). Furthermore, P450 activity is directly related to the concentration of the CPR-P450 complex (Murataliev et al., 2008), whose dissociation constant depends on the structure of each P450. Consequently, the D384Y mutation may have a greater effect on P450s that specifically metabolize pyridaben and tebufenpyrad.

It remains unclear from X-ray crystallography alone how the D384Y mutation can affect P450 activity. The position of D384 on the surface of the protein in the connecting domain of CPR would rule out an effect on FAD, FMN or NADP(H) binding. D384 is also located far from the short hinge region that allows the approximately 90-degree rotation of the FMN domain away from the FAD-linker domain seen between the open and closed conformations of CPR (Aigrain et al., 2009; Hamdane et al., 2009). It does not point towards the space expected to be occupied by P450s in the open conformation of CPR, and superimposition of the open and closed structures indicates little if any movement of the residue at position D384. These considerations rule out a major effect on FAD to FMN to P450 electron transfer. The connecting domain and helix I of CPR are also predicted to remain distant from the ER membrane surface in either open or closed conformations (Laursen et al., 2011). The D384Y mutation has not been documented in human variants of CPR (where the homologous mutation would be E394Y), and the closest human variants S397L or E398A are not associated with any known pathology (Burkhard et al., 2017).

The D384Y mutation additionally introduces a YY dipeptide in the structure. The possible pi-stacking (McGaughey et al., 1998) of the two adjacent aromatic rings might affect protein stability, or cause subtle long-range changes in conformational dynamics which are known to take place during catalysis (Murataliev and Feyereisen, 2000). Moreover, the solution structure of the CPR may differ from the crystal structure in subtle ways (Huang et al., 2013). A model of the extended (open) conformation of human CPR based on solution NMR and small angle X-ray scattering experiments indicates that four residues of helix I of the connecting domain, including the homologous Q391, make polar interactions with the FMN domain (Huang et al., 2013). If this model faithfully represents the changes in the structure of CPR during catalysis, then the most likely explanation for an effect of the D384Y mutation would be a subtle change in the stability of the interaction between the connecting domain and the FMN domain in the open conformation, which is the conformation in which electrons are transferred from FMN to P450s.

Given the conservation of sequence, the homologous mutation to D384Y would be E395Y in *D. melanogaster*. Therefore, the fly may be suitable for studying the effect of the mutation *in vivo* by a reverse genetic approach using CRISPR-Cas9 technology combined with homologous recombination-directed gene modification. An intriguing possibility to explore is that the D384Y mutation has a fitness cost to mites that are not exposed to pesticides. The BSA peak centering on the mutation results not from elevated MR-VP frequency in the acaricide-treated groups, but rather in relatively low MR-VP allele frequencies in mites from control populations (i.e., in the absence of selection, the variant rapidly decreased in allele frequency, Figs. S3B–C); the same pattern was also observed when the genomic region surrounding the allele was associated with spirodiclofen resistance in SR-VP, a different strain of *T. urticae* (Wybouw et al., 2019), in which it was also shown that P450s are involved in spirodiclofen resistance (Demaeght et al., 2013; Van Pottelberge et al., 2009a).

Another protein that may be involved in detoxification by way of P450 regulation is a DBD-lacking NHR96-like gene, *tetur06g04270*, which appears in two tandem copies in both sensitive and resistant parental strains; the genes fall roughly at the center of a minor BSA peak (QTL 3) in the tebufenpyrad-selected group (mites in the pyridaben-selected group also showed increased MR-VP allele frequency in that region, albeit not significantly). Most NHRs are transcription factors; a ligand-binding domain (LBD) interacts with hydrophobic signaling molecules, which then cause the NHR to affect transcription of select genes via its DNA-binding domain (DBD). The two NHR96-like genes are not canonical NHRs as they completely lack the DBD. Further genomic analyses revealed that in addition to the *tetur06g04270* genes, the *T. urticae* genome contains 45 other NHR96-like genes that contained the LBD but were missing the DBD, and that this gene expansion appears to be unique to *T. urticae* (although genome information is not yet available for other spider mite species).

NHRs are diverse and have many functions; they are classified into groups NR0 through NR6, and into subgroups according to their highly conserved domain structure, with non-canonical NHRs that lack either the LBD or the DBD classified as NR0 regardless of origin (Nuclear Receptors Nomenclature Committee, 1999). Our comprehensive search of the NCBI database showed that E75, E78, and FTZ-F1 DBD-lacking NHR-like genes appear to be common in arthropods, but while canonical E75s, E78s and FTZ-F1s are known for their role in metamorphosis, vitellogenesis and embryogenesis (Fahrbach et al., 2012), little is known about the function of DBD-lacking NHR-like genes or how they interact with their targets. In *D. melanogaster*, DBD-lacking E75B acts by heterodimerizing with DHR3 (Reinking et al., 2005), while a DBD-lacking DHR3 plays a role in regulating cell growth by interacting with *Drosophila* ribosomal protein S6 kinase in a yet unknown fashion (Montagne et al., 2010). Since most of the work on arthropod NHRs has been done on *D. melanogaster*, and NHR96-like DBD-lacking genes are only known to be expanded in *T. urticae*, no information is currently available about their potential mode of action. Given *T. urticae*'s polyphagous lifestyle and pest status, a connection between NHR96-like DBD-lacking genes and xenobiotic metabolism is a possibility warranting further exploration, especially considering that *D. melanogaster*'s canonical NHR96 – which has the highest BLASTp match for either copy of *tetur06g04270* – has been implicated in detoxification. Xenobiotic-independent overexpression of NHR96 in *D. melanogaster* L3 larvae induced expression of detoxification genes (King-Jones et al., 2006), and NHR96 overexpression in the Malpighian tubules increased DDT resistance (Afschar et al., 2016). Additionally, adult NHR96 null mutants of *D. melanogaster* were more sensitive to chronic DDT exposure (King-Jones et al., 2006), the sedative effects of phenobarbital (PB) (King-Jones et al., 2006), permethrin (a pyrethroid) (Beaver et al., 2010) and malathion (Afschar et al., 2016). Many of the genes affected by either the NHR96 loss- or gain-of-function mutations encode members of the classic detoxification enzyme families: P450s, glutathione S-transferases (GSTs), carboxylesterases, and UDP-glucuronosyl transferases (UGTs) (King-Jones et al., 2006). These gene families play key roles in detoxification across the animal kingdom, and some – like the P450s – have been expanded in *T. urticae* (Grbić et al., 2011).

5. Conclusion

In this study, we compared and contrasted selection responses to three METI-I acaricides: fenpyroximate, pyridaben, and tebufenpyrad. We found that crossing a resistant strain of *T. urticae* to a susceptible one and separately selecting the offspring with the three acaricides did not yield the same genetic response. While a previously identified H92R target-site mutation was significantly associated with resistance to all three METI-I acaricides, we found that additional loci were associated with resistance to pyridaben and tebufenpyrad, including a genomic region previously associated with spirodiclofen resistance. This region included a variant in CPR, which may be responsible for improving the efficiency of relevant P450s, but at a likely fitness cost in the absence of acaricide treatment. A region connected with resistance to tebufenpyrad included two tandem copies of NHR96-like genes that lacked a DNA-binding domain, and further manual annotation revealed a total of 47 such genes in *T. urticae*. An NCBI database search suggested that an expansion of these genes appears to be unique to *T. urticae*, and their function is currently unknown. Although the role of the CPR mutation and the DBD-lacking NHR96-like genes in xenobiotic resistance in *T. urticae* remain speculative, the link between the associated genetic

regions and resistance to some, but not all, METI-Is, suggests that adaptation to treatment with those acaricides involves different pathways in the spider mite.

Declarations of interests

None.

Acknowledgments

The authors thank Peter Demaeght for the extraction of RNA from the MR-VP strain. We also thank Nicky Wybouw for the maintenance of strains under selection.

Appendix A. Supplementary data

Supplementary data to this article can be found online at https://doi.org/10.1016/j.ibmb.2019.04.011.

Funding

This work was supported by the Research Foundation Flanders [grant numbers G009312N, G053815N], the European Research Council under the European Union's Horizon 2020 research and innovation programme [grant numbers 772026-POLYADAPT, 773902-SUPERPEST], the USA National Science Foundation [grant number 1457346], and the National Institutes of Health Genetics Training [grant number T32GM007464]. WD is a postdoctoral fellow of the Research Foundation Flanders (FWO)Research reported in this publication utilized the High-Throughput Genomics and Bioinformatic Analysis Shared Resource at the Huntsman Cancer Institute at the University of Utah and was supported by the National Cancer Institute of the National Institutes of Health [grant number P30CA042014]. The content is solely the responsibility of the authors and does not necessarily represent the official views of the funding agencies.

References

Abeel, T., Van Parys, T., Saeys, Y., Galagan, J., Van De Peer, Y., 2012. GenomeView: a next-generation genome browser. Nucleic Acids Res. 40, e12. https://doi.org/10.1093/nar/gkr995.

Afschar, S., Toivonen, J.M., Hoffmann, J.M., Tain, L.S., Wieser, D., Finlayson, A.J., Driege, Y., Alic, N., Emran, S., Stinn, J., Froehlich, J., Piper, M.D., Partridge, L., 2016. Nuclear hormone receptor DHR96 mediates the resistance to xenobiotics but not the increased lifespan of insulin-mutant *Drosophila*. Proc. Natl. Acad. Sci. Unit. States Am. 113, 1321–1326. https://doi.org/10.1073/pnas.1515137113.

Aigrain, L., Pompon, D., Moréra, S., Truan, G., 2009. Structure of the open conformation of a functional chimeric NADPH cytochrome P450 reductase. EMBO Rep. 10, 742–747. https://doi.org/10.1038/embor.2009.82.

Angerer, H., Nasiri, H.R., Niedergesäß, V., Kerscher, S., Schwalbe, H., Brandt, U., 2012. Tracing the tail of ubiquinone in mitochondrial complex I. Biochim. Biophys. Acta Bioenerg. 1817, 1776–1784. https://doi.org/10.1016/j.bbabio.2012.03.021.

Bajda, S., Dermauw, W., Panteleri, R., Sugimoto, N., Douris, V., Tirry, L., Osakabe, M., Vontas, J., Van Leeuwen, T., 2017. A mutation in the PSST homologue of complex I (NADH:ubiquinone oxidoreductase) from *Tetranychus urticae* is associated with resistance to METI acaricides. Insect Biochem. Mol. Biol. 80, 79–90. https://doi.org/10.1016/j.ibmb.2016.11.010.

Bateman, A., Martin, M.J., O'Donovan, C., Magrane, M., Apweiler, R., Alpi, E., Antunes, R., Arganiska, J., Bely, B., Bingley, M., Bonilla, C., Britto, R., Bursteinas, B., Chavali, G., Cibrian-Uhalte, E., Da Silva, A., De Giorgi, M., Dogan, T., Fazzini, F., Gane, P., Castro, L.G., Garmiri, P., Hatton-Ellis, E., Hieta, R., Huntley, R., Legge, D., Liu, W., Luo, J., Macdougall, A., Mutowo, P., Nightingale, A., Orchard, S., Pichler, K., Poggioli, D., Pundir, S., Pureza, L., Qi, G., Rosanoff, S., Saidi, R., Sawford, T., Shypitsyna, A., Turner, E., Volynkin, V., Wardell, T., Watkins, X., Zellner, H., Cowley, A., Figueira, L., Li, W., McWilliam, H., Lopez, R., Xenarios, I., Bougueleret, L., Bridge, A., Poux, S., Redaschi, N., Aimo, L., Argoud-Puy, G., Auchincloss, A., Axelsen, K., Bansal, P., Baratin, D., Blatter, M.C., Boeckmann, B., Bolleman, J., Boutet, E., Breuza, L., Casal-Casas, C., De Castro, E., Coudert, E., Cuche, B., Doche, M., Dornevil, D., Duvaud, S., Estreicher, A., Famiglietti, L., Feuermann, M., Gasteiger, E., Gehant, S., Gerritsen, V., Gos, A., Gruaz-Gumowski, N., Hinz, U., Hulo, C., Jungo, F., Keller, G., Lara, V., Lemercier, P., Lieberherr, D., Lombardot, T., Martin, X., Masson, P., Morgat, A., Neto, T., Nouspikel, N., Paesano, S., Pedruzzi, I., Pilbout, S., Pozzato, M., Pruess, M., Rivoire, C., Roechert, B., Schneider, M., Sigrist, C., Sonesson, K., Staehli, S., Stutz, A., Sundaram, S., Tognolli, M., Verbregue, L., Veuthey, A.L., Wu, C.H., Arighi, C.N., Arminski, L., Chen, C., Chen, Y., Garavelli, J.S., Huang, H., Laiho, K., McGarvey, P., Natale, D.A., Suzek, B.E., Vinayaka, C.R., Wang, Q., Wang, Y., Yeh, L.S., Yerramalla, M.S., Zhang, J., 2015. UniProt: a hub for protein information. Nucleic Acids Res. 43, D204–D212. https://doi.org/10.1093/nar/gku989.

Bates, D., Mächler, M., Bolker, B., Walker, S., 2015. Fitting linear mixed-effects models using lme4. J. Stat. Softw. 67, 51. https://doi.org/10.18637/jss.v067.i01.

Beaver, L.M., Hooven, L.A., Butcher, S.M., Krishnan, N., Sherman, K.A., Chow, E.S.Y., Giebultowicz, J.M., 2010. Circadian clock regulates response to pesticides in *Drosophila* via conserved Pdp1 pathway. Toxicol. Sci. 115, 513–520. https://doi.org/10.1093/toxsci/kfq083.

Bryon, A., Kurlovs, A.H., Dermauw, W., Greenhalgh, R., Riga, M., Grbić, M., Tirry, L., Osakabe, M., Vontas, J., Clark, R.M., Van Leeuwen, T., 2017. Disruption of a horizontally transferred phytoene desaturase abolishes carotenoid accumulation and diapause in *Tetranychus urticae*. Proc. Natl. Acad. Sci. Unit. States Am. 114, E5871–E5880. https://doi.org/10.1073/pnas.1706865114.

Burkhard, F.Z., Parween, S., Udhane, S.S., Flück, C.E., Pandey, A.V., 2017. P450 Oxidoreductase deficiency: analysis of mutations and polymorphisms. J. Steroid Biochem. Mol. Biol. 165, 38–50. https://doi.org/10.1016/J.JSBMB.2016.04.003.

Chaisson, M.J., Tesler, G., 2012. Mapping single molecule sequencing reads using basic local alignment with successive refinement (BLASR): application and theory. BMC Bioinf. 13, 238. https://doi.org/10.1186/1471-2105-13-238.

Cheng, D., Xia, Q., Duan, J., Wei, L., Huang, C., Li, Z., Wang, G., Xiang, Z., 2008. Nuclear receptors in *Bombyx mori*: insights into genomic structure and developmental expression. Insect Biochem. Mol. Biol. 38, 1130–1137. https://doi.org/10.1016/j.ibmb.2008.09.013.

Cho, J.B., Kim, Y.J., Ahn, Y.J., Yoo, J.K., Lee, J.O., 1995. Monitoring of acaricide resistance in field-collected populations of *Tetranychus urticae* (Acari: Tetranychidae) in Korea. Kor. J. Appl. Entomol. 34, 40–45.

Cingolani, P., Platts, A., Wang, L.L., Coon, M., Nguyen, T., Wang, L., Land, S.J., Lu, X., Ruden, D.M., 2012. A program for annotating and predicting the effects of single nucleotide polymorphisms, SnpEff: SNPs in the genome of *Drosophila melanogaster* strain w 1118 ; Fly 6, 80–92. iso-2; iso-3. https://doi.org/10.4161/fly.19695.

Degli Esposti, M., 1998. Inhibitors of NADH-ubiquinone reductase: an overview. Biochim. Biophys. Acta Bioenerg. 1364, 222–235. https://doi.org/10.1016/S0005-2728(98)00029-2.

Demaeght, P., Dermauw, W., Tsakireli, D., Khajehali, J., Nauen, R., Tirry, L., Vontas, J., Lümmen, P., Van Leeuwen, T., 2013. Molecular analysis of resistance to acaricidal spirocyclic tetronic acids in *Tetranychus urticae*: CYP392E10 metabolizes spirodiclofen, but not its corresponding enol. Insect Biochem. Mol. Biol. 43, 544–554. https://doi.org/10.1016/j.ibmb.2013.03.007.

Demaeght, P., Osborne, E.J., Odman-Naresh, J., Grbić, M., Nauen, R., Merzendorfer, H., Clark, R.M., Van Leeuwen, T., 2014. High resolution genetic mapping uncovers chitin synthase-1 as the target-site ofthe structurally diverse mite growth inhibitors clofentezine, hexythiazox and etoxazole in *Tetranychus urticae*. Insect Biochem. Mol. Biol. 51, 52–61. https://doi.org/10.1016/j.ibmb.2014.05.004.

Dermauw, W., Wybouw, N., Rombauts, S., Menten, B., Vontas, J., Grbic, M., Clark, R.M., Feyereisen, R., Van Leeuwen, T., 2013. A link between host plant adaptation and pesticide resistance in the polyphagous spider mite *Tetranychus urticae*. Proc. Natl. Acad. Sci. U. S. A 110, E113–E122. https://doi.org/10.1073/pnas.1213214110.

Devine, G.J., Barber, M., Denholm, I., 2001. Incidence and inheritance of resistance to METI-acaricides in European strains of the two-spotted spider mite (*Tetranychus urticae*) (Acari: Tetranychidae). Pest Manag. Sci. 57, 443–448. https://doi.org/10.1002/ps.307.

Dobin, A., Davis, C.A., Schlesinger, F., Drenkow, J., Zaleski, C., Jha, S., Batut, P., Chaisson, M., Gingeras, T.R., 2013. STAR: Ultrafast universal RNA-seq aligner. Bioinformatics 29, 15–21. https://doi.org/10.1093/bioinformatics/bts635.

Duarte, M., Pópulo, H., Videira, A., Friedrich, T., Schulte, U., 2002. Disruption of iron-sulphur cluster N2 from NADH: ubiquinone oxidoreductase by site-directed mutagenesis. Biochem. J. 364, 833–839. https://doi.org/10.1042/BJ20011750.

Fahrbach, S.E., Smagghe, G., Velarde, R.A., 2012. Insect nuclear receptors. Annu. Rev. Entomol. 57, 83–106. https://doi.org/10.1146/annurev-ento-120710-100607.

Fendel, U., Tocilescu, M.A., Kerscher, S., Brandt, U., 2008. Exploring the inhibitor binding pocket of respiratory complex I. Biochim. Biophys. Acta Bioenerg. 1777, 660–665. https://doi.org/10.1016/j.bbabio.2008.04.033.

Feyereisen, R., 2015. Insect P450 inhibitors and insecticides: challenges and opportunities. Pest Manag. Sci. 71, 793–800. https://doi.org/10.1002/ps.3895.

Feyereisen, R., Dermauw, W., Van Leeuwen, T., 2015. Genotype to phenotype, the molecular and physiological dimensions of resistance in arthropods. Pestic. Biochem. Physiol. 121, 61–77. https://doi.org/10.1016/j.pestbp.2015.01.004.

Fiedorczuk, K., Letts, J.A., Degliesposti, G., Kaszuba, K., Skehel, M., Sazanov, L.A., 2016. Atomic structure of the entire mammalian mitochondrial complex I. Nature 538, 406–410. https://doi.org/10.1038/nature19794.

Finn, R.D., Coggill, P., Eberhardt, R.Y., Eddy, S.R., Mistry, J., Mitchell, A.L., Potter, S.C., Punta, M., Qureshi, M., Sangrador-Vegas, A., Salazar, G.A., Tate, J., Bateman, A., 2016. The Pfam protein families database: towards a more sustainable future. Nucleic Acids Res. 44, D279–D285. https://doi.org/10.1093/nar/gkv1344.

Friedrich, T., 1998. The NADH:ubiquinone oxidoreductase (complex I) from *Escherichia coli*. Biochim. Biophys. Acta Bioenerg. 1364, 134–146. https://doi.org/10.1016/S0005-2728(98)00024-3.

Gasteiger, E., Gattiker, A., Hoogland, C., Ivanyi, I., Appel, R.D., Bairoch, A., 2003. ExPASy: the proteomics server for in-depth protein knowledge and analysis. Nucleic Acids Res. 31, 3784–3788. https://doi.org/10.1093/nar/gkg563.

Grbić, M., Van Leeuwen, T., Clark, R.M., Rombauts, S., Rouzé, P., Grbić, V., Osborne, E.J., Dermauw, W., Ngoc, T., Cao, P., Ortego, F., Hernández-Crespo, P., Diaz, I., Martinez, M., Navajas, M., Sucena, É., Magalhães, S., Nagy, L., Pace, R.M., Djuranović, S., Smagghe, G., Iga, M., Christiaens, O., Veenstra, J. a., Ewer, J., Villalobos, R.M.,

Hutter, J.L., Hudson, S.D., Velez, M., Yi, S.V., Zeng, J., Pires-daSilva, A., Roch, F., Cazaux, M., Navarro, M., Zhurov, V., Acevedo, G., Bjelica, A., Fawcett, J.a., Bonnet, E., Martens, C., Baele, G., Wissler, L., Sanchez-Rodriguez, A., Tirry, L., Blais, C., Demeestere, K., Henz, S.R., Gregory, T.R., Mathieu, J., Verdon, L., Farinelli, L., Schmutz, J., Lindquist, E., Feyereisen, R., Van de Peer, Y., Ngoc, P.C.T., Ortego, F., Hernández-Crespo, P., Diaz, I., Martinez, M., Navajas, M., Sucena, É., Magalhães, S., Nagy, L., Pace, R.M., Djuranović, S., Smagghe, G., Iga, M., Christiaens, O., Veenstra, J. a., Ewer, J., Villalobos, R.M., Hutter, J.L., Hudson, S.D., Velez, M., Yi, S.V., Zeng, J., Pires-daSilva, A., Roch, F., Cazaux, M., Navarro, M., Zhurov, V., Acevedo, G., Bjelica, A., Fawcett, J.a., Bonnet, E., Martens, C., Baele, G., Wissler, L., Sanchez-Rodriguez, A., Tirry, L., Blais, C., Demeestere, K., Henz, S.R., Gregory, T.R., Mathieu, J., Verdon, L., Farinelli, L., Schmutz, J., Lindquist, E., Feyereisen, R., Van de Peer, Y., 2011. The genome of *Tetranychus urticae* reveals herbivorous pest adaptations. Nature 479, 487–492. https://doi.org/10.1038/nature10640.

Hamdane, D., Xia, C., Im, S.C., Zhang, H., Kim, J.J.P., Waskell, L., 2009. Structure and function of an NADPH-cytochrome P450 oxidoreductase in an open conformation capable of reducing cytochrome P450. J. Biol. Chem. 284, 11374–11384. https://doi.org/10.1074/jbc.M807868200.

Herron, G.A., Rophail, J., 1998. Tebufenpyrad (Pyranica®) resistance detected in two-spotted spider mite *Tetranychus urticae* Koch (Acari: Tetranychidae) from apples in Western Australia. Exp. Appl. Acarol. 22, 633–641. https://doi.org/10.1023/A:1006058705429.

Hollingworth, R.M., Ahammadsahib, K.I., 1995. Inhibitors of respiratory complex I. Mechanisms, pesticidal actions and toxicology. Rev. Pestic. Toxicol. 3, 277–302.

Hollingworth, R.M., Ahammadsahib, K.I., Gadelhak, G., McLaughlin, J.L., 1994. New inhibitors of complex I of the mitochondrial electron transport chain with activity as pesticides. Biochem. Soc. Trans. 22, 230–233. https://doi.org/10.1042/BST0220230.

Huang, W.C., Ellis, J., Moody, P.C.E., Raven, E.L., Roberts, G.C.K., 2013. Redox-linked domain movements in the catalytic cycle of cytochrome P450 reductase. Structure 21, 1581–1589. https://doi.org/10.1016/j.str.2013.06.022.

Huerta-Cepas, J., Serra, F., Bork, P., 2016. ETE 3: reconstruction, analysis, and visualization of phylogenomic data. Mol. Biol. Evol. 33, 1635–1638. https://doi.org/10.1093/molbev/msw046.

Karp, G., 2008. Cell and Molecular Biology, fifth ed. Wiley.

Katoh, K., Misawa, K., Kuma, K., Miyata, T., 2002. MAFFT: a novel method for rapid multiple sequence alignment based on fast Fourier transform. Nucleic Acids Res. 30, 3059–3066. https://doi.org/10.1093/nar/gkf436.

Kelley, L.A., Mezulis, S., Yates, C.M., Wass, M.N., Sternberg, M.J.E., 2015. The Phyre2 web portal for protein modeling, prediction and analysis. Nat. Protoc. 10, 845–858. https://doi.org/10.1038/nprot.2015.053.

King-Jones, K., Horner, M.A., Lam, G., Thummel, C.S., 2006. The DHR96 nuclear receptor regulates xenobiotic responses in *Drosophila*. Cell Metabol. 4, 37–48. https://doi.org/10.1016/j.cmet.2006.06.006.

King-Jones, K., Thummel, C.S., 2005. Nuclear receptors - a perspective from *Drosophila*. Nat. Rev. Genet. 6, 311–323. https://doi.org/10.1038/nrg1581.

Kwon, D.H., Clark, J.M., Lee, S.H., 2010. Extensive gene duplication of acetylcholinesterase associated with organophosphate resistance in the two-spotted spider mite. Insect Mol. Biol. 19, 195–204. https://doi.org/10.1111/j.1365-2583.2009.00958.x.

Larkin, M.A., Blackshields, G., Brown, N.P., Chenna, R., Mcgettigan, P.A., McWilliam, H., Valentin, F., Wallace, I.M., Wilm, A., Lopez, R., Thompson, J.D., Gibson, T.J., Higgins, D.G., 2007. Clustal W and clustal X version 2.0. Bioinformatics 23, 2947–2948. https://doi.org/10.1093/bioinformatics/btm404.

Laursen, T., Jensen, K., Møller, B.L., 2011. Conformational changes of the NADPH-dependent cytochrome P450 reductase in the course of electron transfer to cytochromes P450. Biochim. Biophys. Acta Protein Proteonomics 1814, 132–138. https://doi.org/10.1016/j.bbapap.2010.07.003.

Li, H., Durbin, R., 2009. Fast and accurate short read alignment with Burrows-Wheeler transform. Bioinformatics 25, 1754–1760. https://doi.org/10.1093/bioinformatics/btp324.

Li, H., Handsaker, B., Wysoker, A., Fennell, T., Ruan, J., Homer, N., Marth, G., Abecasis, G., Durbin, R., 2009. The sequence alignment/map format and SAMtools. Bioinformatics 25, 2078–2079. https://doi.org/10.1093/bioinformatics/btp352.

Li, X., Schuler, M. a, Berenbaum, M.R., 2007. Molecular mechanisms of metabolic resistance to synthetic and natural xenobiotics. Annu. Rev. Entomol. 52, 231–253. https://doi.org/10.1146/annurev.ento.51.110104.151104.

Lümmen, P., 2007. Mitochondrial electron transport complexes as biochemical target sites for insecticides and acaricids. In: Insecticides Design Using Advanced Technologies. Springer, Berlin, Heidelberg, pp. 197–215. https://doi.org/10.1007/978-3-540-46907-0_8.

Lümmen, P., 1998. Complex I inhibitors as insecticides and acaricides. Biochim. Biophys. Acta Bioenerg. 1364, 287–296. https://doi.org/10.1016/S0005-2728(98)00034-6.

Magnitsky, S., Toulokhonova, L., Yano, T., Sled, V.D., Hägerhäll, C., Grivennikova, V.G., Burbaev, D.S., Vinogradov, A.D., Ohnishi, T., 2002. EPR characterization of ubisemiquinones and iron-sulfur cluster N2, central components of the energy coupling in the NADH-ubiquinone oxidoreductase (complex I) in situ. J. Bioenerg. Biomembr. 34, 193–208. https://doi.org/10.1023/A:1016083419979.

McGaughey, G.B., Gagne, M., Rappe, A.K., 1998. Pi-stacking interactions. J. Biol. Chem. 273, 15458–15463. https://doi.org/10.1074/jbc.273.25.15458.

McKenna, A., Hanna, M., Banks, E., Sivachenko, A., Cibulskis, K., Kernytsky, A., Garimella, K., Altshuler, D., Gabriel, S., Daly, M., DePristo, M.A., 2010. The genome analysis toolkit: a MapReduce framework for analyzing next-generation DNA sequencing data. Genome Res. 20, 1297–1303. https://doi.org/10.1101/gr.107524.110.

Michigan State University Arthropod pesticide resistance database. n.d [WWW Document]. URL. https://www.pesticideresistance.org/display.php?page=species&arId=536, Accessed date: 12 June 2018.

Migeon, A., Nouguier, E., Dorkeld, F., 2018. Spider mites web: a comprehensive database for the Tetranychidae. In: Trends in Acarology. Springer, Dordrecht, pp. 557–560. https://doi.org/10.1007/978-90-481-9837-5_96.

Miller, M.A., Pfeiffer, W., Schwartz, T., 2010. Creating the CIPRES science gateway for inference of large phylogenetic trees. In: 2010 Gateway Computing Environments Workshop, GCE 2010. IEEE, New Orleans, LA, USA, pp. 1–8. https://doi.org/10.1109/GCE.2010.5676129.

Montagne, J., Lecerf, C., Parvy, J.P., Bennion, J.M., Radimerski, T., Ruhf, M.L., Zilbermann, F., Vouilloz, N., Stocker, H., Hafen, E., Kozma, S.C., Thomas, G., 2010. The nuclear receptor DHR3 modulates ds6 kinase- dependent growth in *Drosophila*. PLoS Genet. 6, e1000937. https://doi.org/10.1371/journal.pgen.1000937.

Murataliev, M.B., Feyereisen, R., 2000. Interaction of NADP(H) with oxidized and reduced P450 reductase during catalysis. Studies with nucleotide analogues. Biochemistry 39, 5066–5074. https://doi.org/10.1021/bi992917k.

Murataliev, M.B., Feyereisen, R., Walker, F.A., 2004. Electron transfer by diflavin reductases. Biochim. Biophys. Acta Protein Proteonomics 1698, 1–26. https://doi.org/10.1016/j.bbapap.2003.10.003.

Murataliev, M.B., Guzov, V.M., Walker, F.A., Feyereisen, R., 2008. P450 reductase and cytochrome b5 interactions with cytochrome P450: effects on house fly CYP6A1 catalysis. Insect Biochem. Mol. Biol. 38, 1008–1015. https://doi.org/10.1016/j.ibmb.2008.08.007.

Okun, J.G., Lümmen, P., Brandt, U., 1999. Three classes of inhibitors share a common binding domain in mitochondrial complex I (NADH:Ubiquinone oxidoreductase). J. Biol. Chem. 274, 2625–2630. https://doi.org/10.1074/jbc.274.5.2625.

Ozawa, A., 1994. Acaricides susceptibility of Kanzawa spider mite, *Tetranychus kanzawai* KISHIDA (Acarina; Tetranychidae) collected from tea fields in Chuuen and Ogasa district in Shizuoka prefecture. Chagyo Kenkyu Hokoku (Tea Res. Journal) 1–14 (1994). https://doi.org/10.5979/cha.1994.1.

R Developement Core Team, 2015. R: a language and environment for statistical computing. R Found. Stat. Comput. 1, 409. https://doi.org/10.1007/978-3-540-74686-7.

Reinking, J., Lam, M.M.S., Pardee, K., Sampson, H.M., Liu, S., Yang, P., Williams, S., White, W., Lajoie, G., Edwards, A., Krause, H.M., 2005. The *Drosophila* nuclear receptor E75 contains heme and is gas responsive. Cell 122, 195–207. https://doi.org/10.1016/j.cell.2005.07.005.

Riga, M., Bajda, S., Themistokleous, C., Papadaki, S., Palzewicz, M., Dermauw, W., Vontas, J., Leeuwen, T. Van, 2017. The relative contribution of target-site mutations in complex acaricide resistant phenotypes as assessed by marker assisted backcrossing in *Tetranychus urticae*. Sci. Rep. 7, 9202. https://doi.org/10.1038/s41598-017-09054-y.

Riga, M., Myridakis, A., Tsakireli, D., Morou, E., Stephanou, E.G., Nauen, R., Van Leeuwen, T., Douris, V., Vontas, J., 2015. Functional characterization of the *Tetranychus urticae* CYP392A11, a cytochrome P450 that hydroxylates the METI acaricides cyenopyrafen and fenpyroximate. Insect Biochem. Mol. Biol. 65, 91–99. https://doi.org/10.1016/j.ibmb.2015.09.004.

Robinson-Rechavi, M., Escriva, H., Laudet, V., 2003. The nuclear receptor superfamily. J. Cell Sci. 116, 585–586. https://doi.org/10.1242/jcs.00247.

Robinson, J.T., Thorvaldsdóttir, H., Winckler, W., Guttman, M., Lander, E.S., Getz, G., Mesirov, J.P., 2011. Integrative genomics viewer. Nat. Biotechnol. 29, 24–26. https://doi.org/10.1038/nbt.1754.

Schuler, F., Casida, J.E., 2001. Functional coupling of PSST and ND1 subunits in NADH:ubiquinone oxidoreductase established by photoaffinity labeling. Biochim. Biophys. Acta Bioenerg. 1506, 79–87. https://doi.org/10.1016/S0005-2728(01)00183-9.

Shiraishi, Y., Murai, M., Sakiyama, N., Ifuku, K., Miyoshi, H., 2012. Fenpyroximate binds to the interface between PSST and 49 kDa subunits in mitochondrial NADH-Ubiquinone oxidoreductase. Biochemistry 51, 1953–1963. https://doi.org/10.1021/bi300047h.

Stamatakis, A., 2014. RAxML version 8: a tool for phylogenetic analysis and post-analysis of large phylogenies. Bioinformatics 30, 1312–1313. https://doi.org/10.1093/bioinformatics/btu033.

Sterck, L., Billiau, K., Abeel, T., Rouzé, P., Van de Peer, Y., 2012. ORCAE: online resource for community annotation of eukaryotes. Nat. Methods 9, 1041. https://doi.org/10.1038/nmeth.2242.

Tamura, K., Stecher, G., Peterson, D., Filipski, A., Kumar, S., 2013. MEGA6: molecular evolutionary genetics analysis version 6.0. Mol. Biol. Evol. 30, 2725–2729. https://doi.org/10.1093/molbev/mst197.

Thomson, S.A., Baldwin, W.S., Wang, Y.H., Kwon, G., LeBlanc, G.A., 2009. Annotation, phylogenetics, and expression of the nuclear receptors in *Daphnia pulex*. BMC Genomics 10, 500. https://doi.org/10.1186/1471-2164-10-500.

Tocilescu, M.A., Fendel, U., Zwicker, K., Dröse, S., Kerscher, S., Brandt, U., 2010. The role of a conserved tyrosine in the 49-kDa subunit of complex I for ubiquinone binding and reduction. Biochim. Biophys. Acta Bioenerg. 1797, 625–632. https://doi.org/10.1016/j.bbabio.2010.01.029.

Udhane, S.S., Parween, S., Kagawa, N., Pandey, A.V., 2017. Altered CYP19A1 and CYP3A4 activities due to mutations A115V, T142A, Q153R and P284L in the human P450 oxidoreductase. Front. Pharmacol. 25, 580. https://doi.org/10.3389/fphar.2017.00580.

Van der Auwera, G.A., Carneiro, M.O., Hartl, C., Poplin, R., del Angel, G., Levy-Moonshine, A., Jordan, T., Shakir, K., Roazen, D., Thibault, J., Banks, E., Garimella, K.V., Altshuler, D., Gabriel, S., DePristo, M.A., 2013. From fastQ data to high-confidence variant calls: the genome analysis toolkit best practices pipeline. Curr. Protoc. Bioinf. 43 11.10.1-11.10.33. https://doi.org/10.1002/0471250953.bi1110s43.

Van Leeuwen, T., Demaeght, P., Osborne, E.J., Dermauw, W., Gohlke, S., Nauen, R., Grbic, M., Tirry, L., Merzendorfer, H., Clark, R.M., 2012. Population bulk segregant mapping uncovers resistance mutations and the mode of action of a chitin synthesis

inhibitor in arthropods. Proc. Natl. Acad. Sci. U.S.A. 109, 4407–4412. https://doi.org/10.1073/pnas.1200068109.

Van Leeuwen, T., Dermauw, W., 2016. The molecular evolution of xenobiotic metabolism and resistance in chelicerate mites. Annu. Rev. Entomol. 61, 475–498. https://doi.org/10.1146/annurev-ento-010715-023907.

Van Leeuwen, T., Stillatus, V., Tirry, L., 2004. Genetic analysis and cross-resistance spectrum of a laboratory-selected chlorfenapyr resistant strain of two-spotted spider mite (Acari: Tetranychidae). Exp. Appl. Acarol. 32, 249–261. https://doi.org/10.1023/B:APPA.0000023240.01937.6d.

Van Leeuwen, T., Tirry, L., Yamamoto, A., Nauen, R., Dermauw, W., 2014. The economic importance of acaricides in the control of phytophagous mites and an update on recent acaricide mode of action research. Pestic. Biochem. Physiol. 121, 12–21. https://doi.org/10.1016/j.pestbp.2014.12.009.

Van Leeuwen, T., Vanholme, B., Van Pottelberge, S., Van Nieuwenhuyse, P., Nauen, R., Tirry, L., Denholm, I., 2008. Mitochondrial heteroplasmy and the evolution of insecticide resistance: non-Mendelian inheritance in action. Proc. Natl. Acad. Sci. U. S. A 105, 5980–5985. https://doi.org/10.1073/pnas.0802224105.

Van Petegem, K., Moerman, F., Dahirel, M., Fronhofer, E.A., Vandegehuchte, M.L., Van Leeuwen, T., Wybouw, N., Stoks, R., Bonte, D., 2018. Kin competition accelerates experimental range expansion in an arthropod herbivore. Ecol. Lett. 21, 225–234. https://doi.org/10.1111/ele.12887.

Van Pottelberge, S., Van Leeuwen, T., Khajehali, J., Tirry, L., 2009a. Genetic and biochemical analysis of a laboratory-selected spirodiclofen-resistant strain of *Tetranychus urticae* Koch (Acari: Tetranychidae). Pest Manag. Sci. 65, 358–366. https://doi.org/10.1002/ps.1698.

Van Pottelberge, S., Van Leeuwen, T., Nauen, R., Tirry, L., 2009b. Resistance mechanisms to mitochondrial electron transport inhibitors in a field-collected strain of *Tetranychus urticae* Koch (Acari: Tetranychidae). Bull. Entomol. Res. 99, 23–31. https://doi.org/10.1017/S0007485308006081.

Vinothkumar, K.R., Zhu, J., Hirst, J., 2014. Architecture of mammalian respiratory complex I. Nature 515, 80–84. https://doi.org/10.1038/nature13686.

Wang, M., Roberts, D., 1997. Three-dimensional structure of NADPH–cytochrome P450 reductase: prototype for FMN-and FAD-containing enzymes. Proc. Natl. Acad. Sci. U. S. A 94, 8411–8416. https://doi.org/10.1073/pnas.94.16.8411.

Wickham, H., 2009. ggplot2 elegant graphics for data analysis. Media 35, 211. https://doi.org/10.1007/978-0-387-98141-3.

Wirth, C., Brandt, U., Hunte, C., Zickermann, V., Zick, V., 2016. Structure and function of mitochondrial complex I. BBA - Bioenerg 1857, 902–914. https://doi.org/10.1016/j.bbabio.2016.02.013.

Wybouw, N., Kosterlitz, O., Kurlovs, A.H., Bajda, S., Greenhalgh, R., Snoeck, S., Bui, H., Bryon, A., Dermauw, W., Van Leeuwen, T., Clark, R.M., 2019. Long-Term population studies uncover the genome structure and genetic basis of xenobiotic and host plant adaptation in the herbivore Tetranychus urticae. Genetics 211, 1409–1427. https://doi.org/10.1534/genetics.118.301803.

Zdobnov, E.M., Apweiler, R., 2001. InterProScan - an integration platform for the signature-recognition methods in InterPro. Bioinformatics 17, 847–848. https://doi.org/10.1093/bioinformatics/17.9.847.

Zickermann, V., Wirth, C., Nasiri, H., Siegmund, K., Schwalbe, H., Hunte, C., Brandt, U., 2015. Mechanistic insight from the crystal structure of mitochondrial complex I. Science (80- 347, 44–49. https://doi.org/10.1126/science.1259859.